

Novel Acetylcholine and Carbamoylcholine Analogues: Development of a Functionally Selective $\alpha_4\beta_2$ Nicotinic Acetylcholine Receptor Agonist

Camilla P. Hansen,[#] Anders A. Jensen,^{*,#} Jeppe K. Christensen,[†] Thomas Balle,[#] Tommy Liljefors,[#] and Bente Frølund^{*,#}

Department of Medicinal Chemistry, Faculty of Pharmaceutical Sciences, University of Copenhagen, Universitetsparken 2, DK-2100 Copenhagen Ø, Denmark, and Department of Receptor Pharmacology, Neurosearch A/S, Pederstrupvej 93, DK-2750 Ballerup, Denmark

Received December 25, 2007

A series of carbamoylcholine and acetylcholine analogues were synthesized and characterized pharmacologically at neuronal nicotinic acetylcholine receptors (nAChRs). Several of the compounds displayed low nanomolar binding affinities to the $\alpha_4\beta_2$ nAChR and pronounced selectivity for this subtype over $\alpha_3\beta_4$, $\alpha_4\beta_4$, and α_7 nAChRs. The high nAChR activity of carbamoylcholine analogue **5d** was found to reside in its *R*-enantiomer, a characteristic most likely true for all other compounds in the series. Interestingly, the pronounced $\alpha_4\beta_2$ selectivities exhibited by some of the compounds in the binding assays translated into functional selectivity. Compound **5a** was a fairly potent partial $\alpha_4\beta_2$ nAChR agonist with negligible activities at the $\alpha_3\beta_4$ and α_7 subtypes, thus being one of the few truly functionally selective $\alpha_4\beta_2$ nAChR agonists published to date. Ligand–protein docking experiments using homology models of the amino-terminal domains of $\alpha_4\beta_2$ and $\alpha_3\beta_4$ nAChRs identified residues Val111(β_2)/Ile113(β_4), Phe119(β_2)/Gln121(β_4), and Thr155(α_4)/Ser150(α_3) as possible key determinants of the $\alpha_4\beta_2/\alpha_3\beta_4$ -selectivity displayed by the analogues.

Introduction

The neurotransmitter acetylcholine (ACh^e) mediates its physiological effects via a plethora of receptors expressed throughout the central nervous system (CNS) and the peripheral nervous system (PNS). These receptors are divided into muscarinic ACh receptors (mAChRs) and nicotinic ACh receptors (nAChRs). Whereas the mAChRs belong to the superfamily of G-protein coupled receptors and mediate the slow metabotropic responses of ACh, the nAChRs are ligand-gated ion channels mediating the fast synaptic transmission of the neurotransmitter.^{1–5}

The nAChRs are localized at presynaptic and postsynaptic neuron terminals, where they mediate the neurotransmission of ACh as well as modulate the activities of other important neurotransmitter systems, including those of dopamine, norepinephrine, serotonin, glutamate, and γ -aminobutyric acid.^{6–12} Hence, the receptors influence many physiological processes and consequently have been proposed to be implicated in a wide range of neurodegenerative and psychiatric disorders such as Alzheimer's disease, Parkinson's disease, epilepsy, schizophrenia, anxiety, and depression. Furthermore, the receptors are important drug targets for smoking cessation aids.^{13–19}

The nAChR complex is assembled by five subunits, and 12 different neuronal receptor subunits, α_2 – α_{10} and β_2 – β_4 , have so far been identified.^{2,20–22} This multiplicity gives rise to a

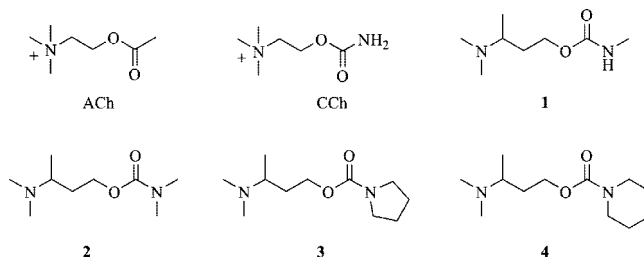


Figure 1. Structures of ACh (acetylcholine), CCh (carbamoylcholine), and selected CCh analogues **1** (3-(dimethylamino)butyl methylcarbamate), **2** (3-(dimethylamino)butyl dimethylcarbamate), **3** (3-(dimethylamino)butyl pyrrolidine-1-carboxylate) and **4** (3-(dimethylamino)butyl piperidine-1-carboxylate).

vast number of possible receptor combinations, and the neuronal nAChRs are either heteromeric complexes formed by α and β subunits (α_9 , α_{10} , or α_2 – α_6 , β_2 – β_4) or homomeric receptors composed of five identical α subunits (α_7 or α_9). However, the majority of the nAChRs in the CNS appears to be heteromeric $\alpha_4\beta_2$ * complexes (the asterisk indicates the possible presence of other subunits) or homomeric α_7 receptors, whereas the $\alpha_3\beta_4$ * subtype is the major ganglionic nAChR.^{1,2} In the heteromeric nAChR, the orthosteric site (i.e., the binding site for ACh) is situated at the interface between an α and a β subunit, whereas the orthosteric site of the homomeric receptor is located at the interface between two neighboring α -subunits.^{3,23,24}

Even though the knowledge and understanding of the nAChRs are expanding, the complexity of ACh neurotransmission is still poorly understood. The development of ligands capable of discriminating between the different nAChR subtypes is therefore of great value in the explorations of the physiological role of the receptors and their potential as therapeutic targets for the above-mentioned disorders.

In recent studies, we have investigated the SARs of carbamoylcholine (CCh) analogues, and this work has resulted in the development of potent nAChR agonists with interesting subtype selectivity profiles^{25,26} (Figure 1). For example, the CCh

* To whom correspondence should be addressed. For A.A.J.: phone, (+45) 35336491; fax, (+45) 35336040; e-mail, aaj@farma.ku.dk. For B.F.: phone, (+45) 35336494; fax, (+45) 35336040; e-mail, bfr@farma.ku.dk.

[#] University of Copenhagen.

[†] Neurosearch A/S.

^a Abbreviations: ACh, acetylcholine; AChBP, acetylcholine binding protein; CCh, carbamoylcholine; CDI, carbonyldiimidazole; CNS, central nervous system; DCVC, dry column vacuum chromatography; DMCC, *N,N*-dimethylcarbamoylcholine; EDC·HCl, 1-[3-(dimethylamino)propyl]-3-ethylcarbodiimide hydrochloride; FC, flash chromatography; FMP, FLIPR membrane potential; HEK, human embryonic kidney; MCC, *N*-methylcarbamoylcholine; MLA, methyllycaconitine; mAChR, muscarinic acetylcholine receptor; nAChR, nicotinic acetylcholine receptor; PNS, peripheral nervous system; SAR, structure–activity relationship; TEVC, two electrode voltage clamp.

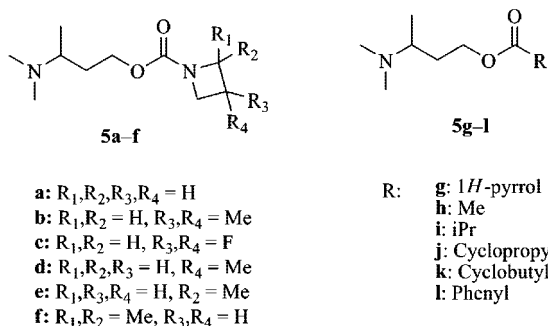


Figure 2. Structures of the ACh and CCh analogues synthesized and characterized in the present study.

analogues **1** and **2** exhibit high selectivities for neuronal nAChRs over muscarinic receptors, and in addition, compound **1** displays a high degree of selectivity toward the $\alpha_4\beta_2$ nAChR subtype over the $\alpha_3\beta_4$ nAChR subtype in binding assays. Different substituents have been introduced at the carbamate nitrogen in the CCh analogue (**2**), and it has been observed that large substituents like propyl or phenyl groups in this position result in significantly decreased binding affinities to the nAChRs.²⁶ In contrast, introduction of smaller substituents such as ethyl groups at the carbamate nitrogen is allowed, as these analogues retain the nanomolar binding affinities at the nAChRs displayed by **1** and **2**.²⁶ Finally, incorporating the carbamate nitrogen into a pyrrolidine or a piperidine ring, giving rise to compounds **3** and **4**, respectively, leads to significantly decreased affinities to the nAChRs compared to those of **1** and **2**.^{25,26} All of the CCh analogues studied to date have been demonstrated to be agonists at the $\alpha_3\beta_4$ nAChR subtype.^{25,26}

In the present study, a new series of CCh analogues (compounds **5a–g** in Figure 2) and ACh analogues (where the carbamate function of the original CCh analogue series has been replaced by an ester group, compounds **5h–l** in Figure 2) have been designed and synthesized, and the pharmacological properties of the compounds have been characterized in binding and functional assays at various nAChR subtypes.

Results

Chemistry. The synthetic approaches to the target compounds **5a–l** are outlined in Schemes 1–3. The key compound, the amino alcohol **7**, was synthesized as previously described by conjugate addition of dimethylamine to ethyl crotonate^{27,28} followed by reduction with LiAlH₄.

In the synthesis of the azetidine analogues **5a–f**, compound **7** was reacted with the acylating agent carbonyldiimidazole (CDI)^{29,30} followed by reaction with the appropriate azetidine to give the target carbamates. The reactions proceeded with full conversion in all cases but one: the formation of **5f**, where the azetidine was more sterically hindered.

The azetidines required for these reactions were either commercially available or synthesized using literature procedures. Azetidine formation has been described by various groups,^{31,32} some of these employing one-pot procedures^{33–35} or formation and then reduction of the corresponding β -lactams.^{36–43} In our case these procedures were not successful, and instead, a more elaborate method was employed, as shown in Scheme 2.

In cases where the starting amino alcohols were not commercially available, the corresponding amino acids were treated sequentially with boron trifluoride–diethyl etherate, borane–dimethyl sulfide complex, and sodium hydroxide, giving the amino alcohols in quantitative yields.⁴⁴ The amino alcohols were

reacted with *p*-toluenesulfonyl chloride and cyclized in the presence of potassium *tert*-butoxide and *tert*-butanol, as described by Vaughan et al.⁴⁵ and Thompson et al.⁴⁶ Deprotection using sodium in *n*-pentanol gave the target compounds in overall yields ranging from 36% to 55%.

Attempts to use the same strategy for the synthesis of **5g** failed. Using either phosgene or CDI gave a complex mixture of products. Instead, compound **5g** was synthesized using a method described by Boger et al.⁴⁷ The anhydride of pyrrole-1-carboxylic acid was prepared from pyrrole-1-carboxylic acid and 1-[3-(dimethylamino)-propyl]-3-ethylcarbodiimide hydrochloride (EDC·HCl), which was then followed by in situ coupling with the sodium salt of the amino alcohol **7**.

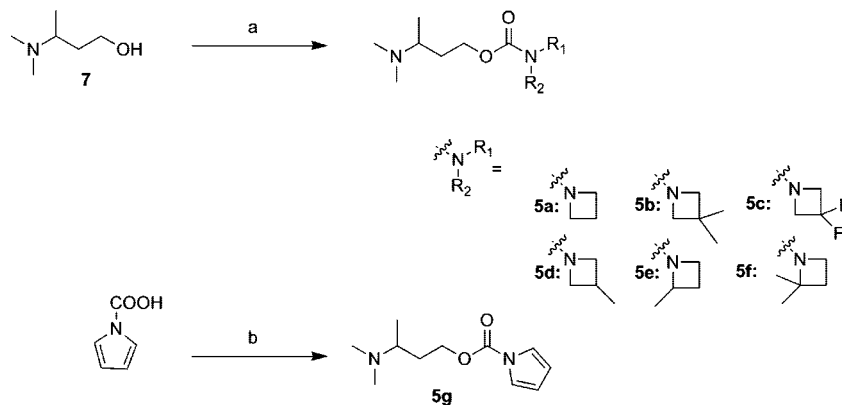
The two enantiomers of **5d** were synthesized following the above-mentioned procedure for **5a–f** using enantiomerically pure (*R*)- and (*S*)-**7**. These amino alcohols were obtained from enantiomerically pure (*R*)- and (*S*)-3-aminobutan-1-ol,⁴⁸ respectively, by reductive amination with formaldehyde and sodium triacetoxyborohydride.^{49,50} The enantiomeric purities of (*R*)-**5d** and (*S*)-**5d** were assessed by ¹H NMR using (*R*)-(-)-2,2,2-trifluoro-1-(9-anthryl)ethanol as the chiral shift reagent (see Supporting Information), and both carbamates were found to be optically pure. Considering the ¹H NMR data and the synthetic route, the carbamates (*R*)-**5d** and (*S*)-**5d** were estimated to have an enantiomeric excess of >95%.

The ester analogues **5h–l** were synthesized as illustrated in Scheme 3 from compound **7** and the appropriate acyl chloride.^{51–53}

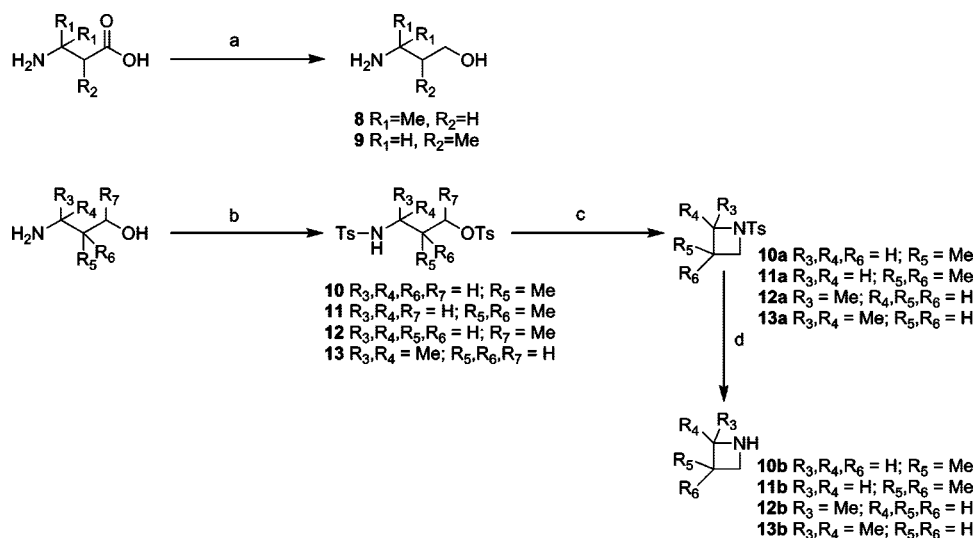
Compounds **5a–k** were isolated as the oxalate salts, whereas ester **5l** was isolated as the hydrochloride salt.

Pharmacology. Binding Properties of Compounds 5a–l to Recombinant nAChRs. The binding properties of compounds **5a–l** were determined in a [³H]epibatidine competition binding assay to heteromeric rat $\alpha_4\beta_2$, $\alpha_3\beta_4$, and $\alpha_4\beta_4$ nAChRs stably expressed in HEK293 cells and in a [³H]MLA competition binding assay to tsA-201 cells transiently transfected with a receptor chimera consisting of the amino-terminal domain of the rat α_7 nAChR and the transmembrane and the intracellular domains of the mouse 5-HT_{3A} receptor (the $\alpha_7/5$ -HT_{3A} chimera). We and others have previously demonstrated that the binding profiles of the $\alpha_4\beta_2$ and the $\alpha_3\beta_4$ cell lines in the [³H]epibatidine binding assay are in excellent agreement with those reported for the recombinant receptors in other studies,^{26,54,55} and the binding properties of the $\alpha_4\beta_4$ nAChR-HEK293 cell line have been characterized by Kellar and co-workers⁵⁴ in a similar [³H]epibatidine binding assay. Furthermore, the binding characteristics of the $\alpha_7/5$ -HT_{3A} chimera in the [³H]MLA binding assay have been shown to be in concordance with those displayed by recombinantly expressed full length α_7 nAChRs and by native α_7 receptors.^{26,56,57}

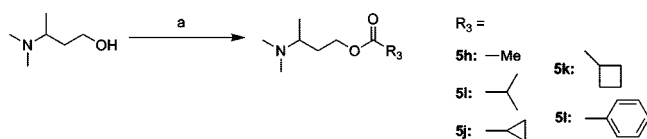
The binding affinities of compounds **5a–l** to the $\alpha_4\beta_2$, $\alpha_3\beta_4$ and $\alpha_4\beta_4$ receptors and the $\alpha_7/5$ -HT_{3A} chimera are presented in Table 1, together with the binding affinities displayed by the reference compounds (*S*)-nicotine and CCh analogues **1**, **2**, **3**, and **4**. The binding profiles of (*S*)-nicotine and compounds **5a–l** at the $\alpha_4\beta_2$, $\alpha_3\beta_4$, and $\alpha_4\beta_4$ nAChR subtypes are shown in Figure 3. As can be seen from Table 1 and Figure 3, the CCh and ACh analogues displayed nano- or micromolar affinity to the heteromeric nAChRs, whereas they either displayed no measurable binding or very weak binding affinities to the $\alpha_7/5$ -HT_{3A} chimera. Several of the compounds displayed significant degrees of selectivity for the $\alpha_4\beta_2$ over the $\alpha_3\beta_4$ nAChR subtype. In the carbamate series **5a–g**, the azetidine analogue **5a** displayed a 2000-fold lower *K_i* value at $\alpha_4\beta_2$ than at $\alpha_3\beta_4$ nAChRs, and this selectivity degree was retained for compounds **5b** and **5c**.

Scheme 1. Synthesis of Carbamates **5a–f** and Pyrrole Analogue **5g**^a

^a (a) CDI, toluene, THF, R₁R₂NH; (b) (1) EDC·HCl, CH₂Cl₂; (2) sodium salt of **7**, THF.

Scheme 2. Synthesis of Azetidines **10b–13b**^a

^a (a) (1) BF₃·OEt₂, THF, reflux; (2) BH₃·SMe₂, reflux; (3) NaOH, reflux; (b) pTsCl, pyridine; (c) ^tBuOK, ^tBuOH; (d) Na, *n*-pentanol, reflux.

Scheme 3. Synthesis of Esters **5h–l**^a

^a (a) R₃COCl, CH₂Cl₂.

An even further increased selectivity degree (11000-fold) was observed for compound **5d** (Table 1).

In contrast to the high $\alpha_4\beta_2/\alpha_3\beta_4$ selectivity ratio observed for the analogues with methyl, dimethyl, and difluoro substituents in the 3-position of the azetidine group, introduction of a methyl substituent in the 2-position of the azetidine ring (**5e**) led to a slightly decreased $\alpha_4\beta_2/\alpha_3\beta_4$ selectivity ratio, and an even more pronounced decrease was observed for the analogue with a double-methylation in this position (**5f**). Finally, the pyrrole analogue (**5g**) displayed lower binding affinities to the three heteromeric nAChRs subtypes than the other CCh analogues where the carbamate nitrogen was incorporated into a ring system, i.e., the azetidine (**5a**), pyrrolidine (**3**), and piperidine (**4**) analogues (Table 1).

In the ACh analogue series, comprising compounds **5h–l**, the cyclopropyl ester **5j** exhibited the highest binding affinity

to $\alpha_4\beta_2$ nAChR, whereas the cyclobutyl analogue **5k** displayed a 25-fold lower affinity to this subtype compared to **5j** (Table 1). Furthermore, compound **5h** (the analogue with closest resemblance to the ACh skeleton) displayed a 17-fold lower binding affinity at the $\alpha_4\beta_2$ subtype than **5j**. In contrast to their different affinities at the $\alpha_4\beta_2$ nAChR subtype, **5h**, **5j**, and **5k** displayed similar *K_i* values at the $\alpha_3\beta_4$ and $\alpha_4\beta_4$ subtypes. Moreover, the ester compounds **5j–l** displayed measurable binding to the $\alpha_7/5$ -HT_{3A} chimera, although the *K_i* values of the compounds were in the high micromolar range (Table 1).

The binding characteristics of the two resolved enantiomers of **5d**, (*R*)-**5d** and (*S*)-**5d**, were determined in order to assess which enantiomer of this CCh analogue possessed the highest nAChR activity. (*R*)-**5d** displayed similar or slightly higher binding affinities to the heteromeric nAChRs than racemic **5d** (Figure 4, Table 1). In contrast, (*S*)-**5d** displayed 27-, 4-, and 27-fold lower binding affinities to the $\alpha_4\beta_2$, $\alpha_3\beta_4$, and $\alpha_4\beta_4$ nAChRs, respectively, than the racemic compound (Figure 4, Table 1).

Functional Characteristics of Compounds 5a–l at the $\alpha_3\beta_4$ nAChR. The functional properties of ACh and compounds **2** and **5a–l** at the $\alpha_3\beta_4$ nAChR-HEK 293 cell line were determined in the FLIPR membrane potential Blue (FMP) assay (Table 2 and Figure 5). This cell line has in previous studies exhibited pharmacological characteristics in the FMP assay in

Table 1. Binding Characteristics of CCh and ACh Analogues to Rat $\alpha_4\beta_2$, $\alpha_3\beta_4$, and $\alpha_4\beta_4$ nAChRs Stably Expressed in HEK293 Cells and to the $\alpha_7/5HT_{3A}$ Chimera Transiently Expressed in tsA201 Cells^a

| | $\alpha_4\beta_2$ -HEK293 | $\alpha_3\beta_4$ -HEK293 | $\alpha_4\beta_4$ -HEK293 | $\alpha_7/5HT_{3A}$ (tsA-201) |
|------------------------|---------------------------|---------------------------|---------------------------|-------------------------------|
| (S)-nicotine | 22 [7.7 ± 0.06] | 600 [6.2 ± 0.04] | 150 [6.8 ± 0.06] | 16000 [4.8 ± 0.02] |
| 1 ^b | 13 [7.9] | 10000 [5.0] | 2600 [5.6] | >1000000 [<3] |
| 2 | 20 [7.7 ± 0.04] | 420 [6.4 ± 0.06] | 150 [6.8 ± 0.04] | >1000000 [<3] |
| 3 | 210 [6.7 ± 0.05] | 25000 [4.6 ± 0.03] | 2200 [5.7 ± 0.04] | >1000000 [<3] |
| 4 | 91 [7.0 ± 0.03] | 2600 [5.6 ± 0.05] | 350 [6.5 ± 0.04] | >1000000 [<3] |
| carbamates | | | | |
| 5a | 5.1 [8.3 ± 0.05] | 11000 [5.0 ± 0.05] | 190 [6.7 ± 0.01] | >1000000 [<3] |
| 5b | 58 [7.2 ± 0.04] | ~300000 [~3.5] | 720 [6.1 ± 0.05] | >1000000 [<3] |
| 5c | 58 [7.2 ± 0.02] | ~100000 [~4] | 1600 [5.8 ± 0.04] | >1000000 [<3] |
| 5d | 2.1 [8.7 ± 0.04] | 23000 [4.6 ± 0.02] | 260 [6.6 ± 0.05] | >1000000 [<3] |
| (R)- 5d | 0.91 [9.0 ± 0.03] | 19000 [4.7 ± 0.02] | 180 [6.7 ± 0.03] | nd |
| (S)- 5d | 57 [7.2 ± 0.05] | ~100000 [~4] | 7100 [5.1 ± 0.05] | nd |
| 5e | 15 [7.8 ± 0.03] | 2500 [5.6 ± 0.02] | 230 [6.6 ± 0.04] | >1000000 [<3] |
| 5f | 210 [6.7 ± 0.06] | 25000 [4.6 ± 0.03] | 3200 [5.5 ± 0.03] | >1000000 [<3] |
| 5g | 310 [6.5 ± 0.06] | ~100000 [~4] | 11000 [5.0 ± 0.03] | >1000000 [<3] |
| esters | | | | |
| 5h | 65 [7.2 ± 0.04] | 4100 [5.4 ± 0.02] | 370 [6.4 ± 0.04] | >1000000 [<3] |
| 5i | 30 [7.5 ± 0.06] | 8500 [5.1 ± 0.04] | 760 [6.1 ± 0.02] | >1000000 [<3] |
| 5j ^c | 3.8 [8.4 ± 0.05] | 4200 [5.4 ± 0.04] | 260 [6.6 ± 0.03] | 280000 [3.6 ± 0.05] |
| 5k ^c | 100 [7.0 ± 0.05] | 3500 [5.5 ± 0.04] | 460 [6.3 ± 0.05] | 290000 [3.5 ± 0.07] |
| 5l ^c | 320 [6.5 ± 0.05] | ~100000 [~4] | 10000 [5.0 ± 0.03] | 190000 [3.7 ± 0.03] |

^a The K_i values are given in nM with $pK_i \pm$ SEM values in brackets. nd, not determined. ^b Binding data for compound **1** is from ref 26. ^c The K_i values for compounds **5j–l** at the $\alpha_7/5HT_{3A}$ chimera are based on estimated IC_{50} values, since neither of the compounds could displace [³H]MLA binding to the chimera completely in the concentrations tested.

good agreement with those observed for the nAChR in conventional electrophysiological setups, in particular when it comes to agonist potencies.²⁶ The 2-methylated azetidinium ring analogue, **5e**, was equipotent to ACh as an $\alpha_3\beta_4$ agonist, displaying an EC_{50} value 4- to 60-fold lower than those for the other compounds in the carbamate series (Table 2 and Figure 5A). In the ester series, the cyclopropyl and cyclobutyl analogues **5j** and **5k** were the more potent agonists (Table 2 and Figure 5B). As can be seen from Figure 5C, a significant correlation ($r^2 = 0.93$) existed between the potencies obtained for compounds **5a–k** at the $\alpha_3\beta_4$ nAChR in the FMP assay and their binding affinities at the receptor in the [³H]epibatidine binding assay.

Functional Characteristics of Compounds 5a and 5d at Human $\alpha_4\beta_2$, $\alpha_3\beta_4$, and α_7 nAChRs. The functional properties of compounds **5a** and **5d** were determined at the human $\alpha_4\beta_2$, $\alpha_3\beta_4$, and α_7 nAChRs expressed in *Xenopus* oocytes using the two-electrode voltage clamp (TEVC) technique (Table 3 and Figure 6). Fully saturated concentration–response curves for the two compounds were only obtained at the $\alpha_4\beta_2$ nAChR. Compound **5a** was a fairly potent partial agonist at the $\alpha_4\beta_2$ nAChR, displaying an EC_{50} value of 7 μ M and a maximal response of 66% of that of ACh. In contrast, the compound only exhibited weak agonistic activity at the $\alpha_3\beta_4$ subtype in concentrations above 100 μ M and was completely inactive at the α_7 nAChR in concentrations up to 320 μ M (Table 3 and Figure 6A). Compound **5d** also displayed negligible activities at the $\alpha_3\beta_4$ and α_7 nAChR at concentrations up to 320 μ M. In contrast to **5a**, however, **5d** was a very low-efficacious partial agonist at the $\alpha_4\beta_2$ nAChR, displaying a maximal response of 9.5% of that of ACh (Table 3 and Figure 6B).

Notably, **5a** and **5d** exhibited significantly higher agonist potencies and, in the case of **5d**, markedly higher efficacy at the rat $\alpha_3\beta_4$ nAChR in the FMP assay than at the human $\alpha_3\beta_4$ nAChR in the TEVC assay (Tables 2 and 3, Figures 5A and 6). These differences may be attributed to the use of $\alpha_3\beta_4$ nAChRs from two different species in the two assays. However, it is more likely that the differences arise from fundamental differences between the assays. First, in the TEVC assay the membrane potential is kept constant during the oocyte record-

ings, which is not the case in the FMP assay. Second, in the FMP assay saturation of the cells with dye may give rise to left-shifted concentration–response curves and to overestimation of the efficacies of the two agonists compared to that of the full agonist ACh. Finally, differences in buffer compositions and/or receptor expression levels in the two assays may also contribute to the observed differences. Several examples exist in the literature where potencies and efficacies obtained for agonists at nAChRs expressed in mammalian cell lines and assayed by fluorescence-based high throughput assays are somewhat higher than those obtained at nAChRs expressed in *Xenopus* oocytes using the TEVC technique.^{26,58–61} Thus, considering the coarse nature of the FMP assay, the conclusions drawn from the functional characterization of ACh and CCh analogues at the $\alpha_3\beta_4$ nAChR in this assay should mainly be focused on the majority of the analogues being agonists at this nAChR subtype and on the general rank order of their agonist potencies. In contrast, electrophysiological recordings at nAChRs expressed in *Xenopus* oocytes give substantially more information about ligand-gated ion channel signaling, and thus, this assay must be considered the golden standard when it comes to studies of nAChRs.

Homology Modeling of the Amino-Terminal Domain of the $\alpha_4\beta_2$ and the $\alpha_3\beta_4$ nAChRs. Homology models of the amino-terminal domains of the $\alpha_4\beta_2$ and the $\alpha_3\beta_4$ nAChRs were employed in order to identify structural determinants for the observed $\alpha_4\beta_2/\alpha_3\beta_4$ selectivities displayed by the CCh and ACh analogues in the binding assays. The homology model of the amino-terminal extracellular domain of the $\alpha_4\beta_2$ receptor reported by Le Novere et al.,⁶² based on the X-ray crystal structure of L-AChBP (from *Lymnaea stagnalis*), was used as a starting point. From this, a model of the orthosteric binding site of the $\alpha_3\beta_4$ receptor was obtained by substitutions of divergent residues in the $\alpha_4\beta_2$ receptor with the corresponding $\alpha_3\beta_4$ residues. The residues of the mature α_4 , α_3 , β_2 and β_4 subunits were numbered according to the sequence alignments in the Uniprot Knowledgebase⁶³ (primary accession number P09483, P04757, P12390, and P12392, respectively).

The dockings of the ACh and CCh analogues to the two receptor models were guided by the binding modes and receptor

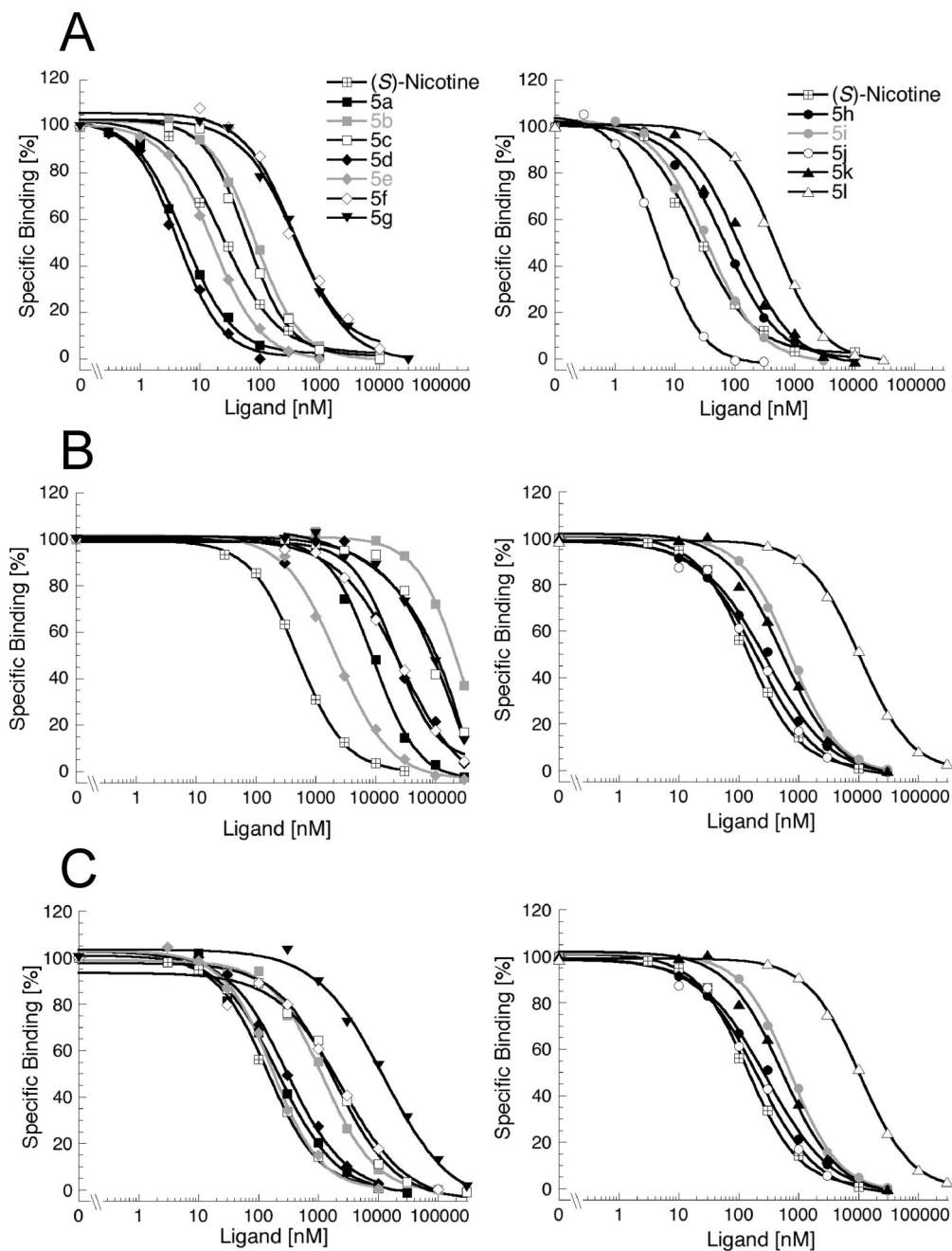


Figure 3. Competition for [^3H]epibatidine binding by (*S*)-nicotine and compounds **5a–I** at heteromeric neuronal nAChRs. Concentration–inhibition curves for carbamates **5a–g** (left column) and esters **5h–I** (right column) at the nAChR subtypes $\alpha_4\beta_2$ (A), $\alpha_3\beta_4$ (B), and $\alpha_4\beta_4$ (C) stably expressed in HEK293 cells in the [^3H]epibatidine binding assay. The binding experiments were performed as described in Experimental Section, and data are given as the mean values of duplicate determinations of single representative experiments (error bars are omitted for reasons of clarity).

interactions displayed by nicotine bound to *L*-AChBP^{23,64} and epibatidine bound to *A*-AChBP (from *Aplysia californica*),^{65,66} given that CCh being a quaternary amine is not optimal as a template.⁶⁴ It is apparent that the mode of binding of epibatidine to *A*-AChBP closely resembles that of nicotine to *L*-AChBP,^{64,66} and the key receptor interactions for nicotine and epibatidine are provided by a protonated sp^3 -hybridized nitrogen atom (cation– π interaction and NH hydrogen bonding) and a pyridyl nitrogen atom (hydrogen bond mediated by a water molecule). As compound **2** also contains the structural elements of hydrogen bonding (i.e., the sp^3 -hybridized nitrogen atom and a carbonyl group), it is reasonable to assume that these are involved in receptor binding of **2** in the same way as the corresponding parts of nicotine and epibatidine. The X-ray structure of epibatidine bound to *A*-AChBP⁶⁶ was chosen as a

template for the bioactive conformation of the parent compound **2**, and Figure 7 displays a low energy conformation of (*R*)-**2** superimposed on the binding conformation of epibatidine. The *R*-enantiomer of **2** was chosen, given that earlier studies have shown this enantiomer to display the highest affinity for the $\alpha_4\beta_2$ and $\alpha_3\beta_4$ nAChRs.²⁵ It is apparent from Figure 7 that compound **2** and epibatidine are of similar size and the key binding elements of epibatidine overlap well with the corresponding parts of (*R*)-**2**. Note that the hydrogen bond accepting pyridyl nitrogen in epibatidine corresponds to the carbonyl oxygen in (*R*)-**2**.

Figure 8 displays compound (*R*)-**2** in its proposed bioactive conformation manually docked into the binding cavities of the homology models of the $\alpha_4\beta_2$ and the $\alpha_3\beta_4$ nAChR. The positively charged nitrogen of (*R*)-**2** is forming a cation– π

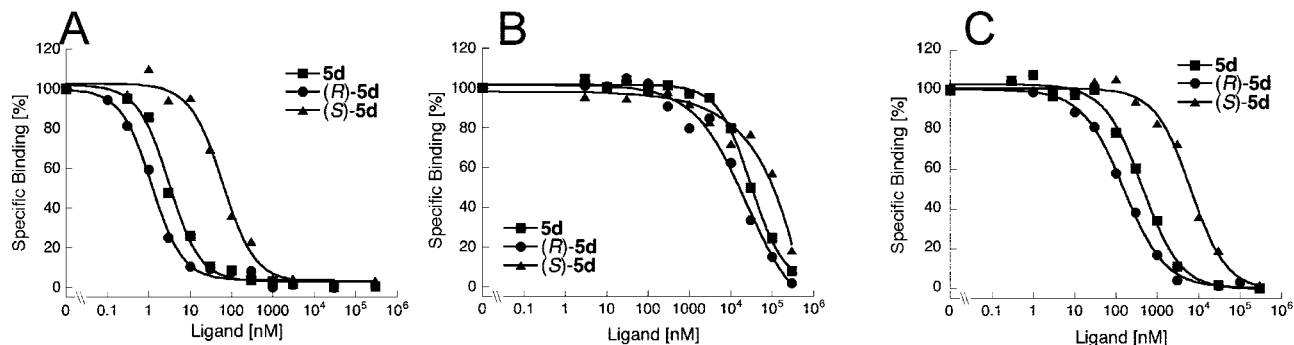


Figure 4. Competition for [^3H]epibatidine binding by **5d** and its two enantiomers (*R*)-**5d** and (*S*)-**5d** at the heteromeric nAChRs $\alpha_4\beta_2$ (A), $\alpha_3\beta_4$ (B), and $\alpha_4\beta_4$ (C) stably expressed in HEK293 cells. The binding experiments were performed as described in Experimental Section, and data are given as mean values of duplicate determinations of single representative experiments (error bars are omitted for reasons of clarity).

Table 2. Functional Characteristics of CCh and ACh Analogues at the Stable $\alpha_3\beta_4$ -HEK293 Cell Line in the FMP Assay^a

| | EC ₅₀ [pEC ₅₀ ± SEM] | R _{max} (% of R _{max} ACh) |
|-----------------------|--|--|
| ACh | 8.9 [5.1 ± 0.03] | 100 |
| 2 | 7.7 [5.1 ± 0.03] | 105 ± 4 |
| carbamates | | |
| 5a | 23 [4.6 ± 0.02] | 106 ± 4 |
| 5b^b | ~300 [3.5] | 43 ± 2 |
| 5c | 95 [4.0 ± 0.03] | 75 ± 3 |
| 5d | 48 [4.3 ± 0.05] | 91 ± 3 |
| 5e | 5.4 [5.3 ± 0.05] | 89 ± 1 |
| 5f | 51 [4.3 ± 0.04] | 90 ± 3 |
| 5g^b | 100–300 [3.5–4] | 27 ± 2 |
| esters | | |
| 5h | 23 [4.6 ± 0.01] | 97 ± 2 |
| 5i | 24 [4.6 ± 0.02] | 100 ± 1 |
| 5j | 7.2 [5.1 ± 0.03] | 105 ± 3 |
| 5k | 8.5 [5.1 ± 0.02] | 85 ± 4 |
| 5l^c | nd | nd |

^a The EC₅₀ values are given in μM with pEC₅₀ ± SEM values in brackets, and the R_{max} values are given as % of the R_{max} of ACh. nd: not determined.

^b The concentration–response curves of **5b** and **5g** did not always reach saturation in the concentration range tested. The responses elicited by 1 mM **5b** and 1 mM **5g** are given as % of R_{max} of ACh, and the EC₅₀ values of the compounds are estimated. ^c **5l** elicited only a weak agonist response at concentrations up to 1 mM, and thus, EC₅₀ and R_{max} values could not be determined.

interaction with Trp154(α_4)/Trp149(α_3) and is enveloped by the aromatic residues Tyr98(α_4)/Tyr93(α_3), Trp154(α_4)/Trp149(α_3), Tyr195(α_4)/Tyr190(α_3), Tyr202(α_4)/Tyr197(α_3), and Trp57(β_2)/Trp59(β_4). The NH⁺ moiety forms a hydrogen bond with the backbone carbonyl of Trp154(α_4)/Trp149(α_3), and an additional hydrogen bond is formed between the carbonyl group of (*R*)-**2** and a water molecule. The water molecule in Figure 8 (shown as a red sphere) is positioned in the same location as the corresponding water molecule in the nicotine–AChBP complex.⁶⁴ In addition, the PASS algorithm⁶⁷ was applied to visualize the cavities and the geometrical proportions of the binding pocket of the $\alpha_4\beta_2$ nAChR. The PASS-contour obtained was filled out nicely by compound (*R*)-**2** (Figure 9), making the docking plausible.

Attempts to dock the *S*-enantiomer of compound **2** using the same manual docking approach were unsuccessful, as they resulted in the C-methyl substituent of (*S*)-**2** exceeding the PASS surface. In addition, a significant steric clash was observed between this C-methyl substituent and the Trp154(α_4)/Trp149(α_3) residues of the $\alpha_4\beta_2$ and the $\alpha_3\beta_4$ receptor (the observed distance between them was 2.6 Å). This may explain the reduced nAChR binding affinity of (*S*)-**2** compared to (*R*)-**2** observed in the binding assays.²⁵

Docking of the series of CCh and ACh analogues, compounds **5a**–**l**, was performed as described for compound **2** using the

proposed bioactive conformation of (*R*)-**2** (Figure 7) as a template. The compounds were docked with the *R*-configuration at the corresponding methyl substituted carbon.

It is of interest to note that when the homology models of the $\alpha_4\beta_2$ and $\alpha_3\beta_4$ nAChRs are compared (Figure 8), the residues of the α_4 and α_3 subunits are fairly similar, whereas the residues of the β_2 and β_4 subunit differ to some extent.^{62,68–70} In the present context, particularly important differences are seen at the Val111(β_2)/Ile113(β_4) and the Phe119(β_2)/Gln121(β_4) residues. It is likely that these residues to some extent are responsible for the receptor selectivities of certain orthosteric ligands. Indeed, in the case of epibatidine, significant differences in binding have been observed when exchanging the Cl atom (which upon docking into the $\alpha_4\beta_2$ homology model points toward the Val111(β_2) residue) with other groups, indicating that hydrophobic and steric interactions of the Val111(β_2) are important upon binding to the $\alpha_4\beta_2$ nAChR.^{71,72}

Discussion

In the present study we have continued our exploration of the CCh analogue as a scaffold in the development of nAChR agonists.^{25,26} In previous studies, the presence of the following structural features of the CCh analogue were found to result in optimal nAChR activity: (1) the presence of a tertiary amino group, (2) a distance of three carbon atoms between the amino and the carbamate group, (3) no substituents at the C-1 and C-2 carbons, and (4) the presence of a single methyl group at the C-3 carbon.^{25,26} Furthermore, the nAChR activities of compounds **1** and **2** were shown to reside primarily in the (*R*)-enantiomer of the racemate.²⁵ Finally, the pharmacological implications of introducing various alkyl and aryl substituents at the carbamate nitrogen of the CCh analogue have been investigated. Introduction of small substituents such as hydrogen, methyl, or ethyl groups in this position of the CCh analogue gave rise to compounds with high nAChR affinities, whereas introduction of larger substituents like propyl or phenyl groups as well as incorporation of the carbamate nitrogen into a pyrrolidine or a piperidine ring (compounds **3** and **4**, respectively) resulted in CCh analogues with moderate to weak nAChR affinities.^{25,26} Interestingly, the substitution pattern at the carbamate nitrogen appeared to be an important determinant of nAChR subtype selectivity, as the monomethylated CCh analogue **1** displayed a significant preference for β_2 -containing nAChRs over β_4 -containing subtypes, whereas the dimethylated analogue **2** did not.²⁶

In the present study we have continued to elucidate the role of the carbamate function in the CCh analogue by designing and synthesizing a series of compounds where the nitrogen has

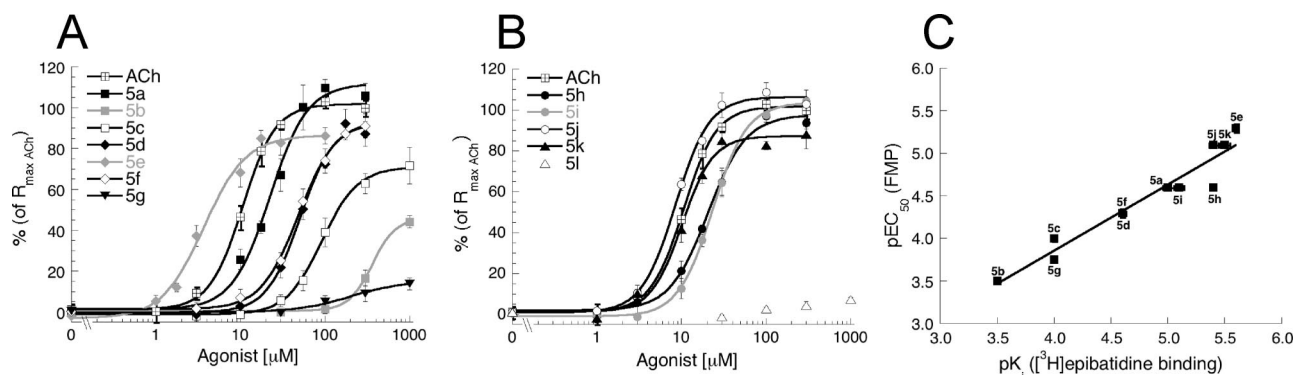


Figure 5. Functional profiles of ACh and compounds **5a–l** at the $\alpha_3\beta_4$ nAChR in the FMP assay. The agonist responses induced by CCh analogues **5a–g** (A) and ACh analogues **5h–l** (B) at the $\alpha_3\beta_4$ nAChR-HEK293 cell line are given as % of the R_{\max} of ACh. Data are the mean \pm SD of duplicate determinations of single representative experiments. (C) Correlation between binding affinities and functional potencies of compounds **5a–k** at the $\alpha_3\beta_4$ -HEK293 cell line.

Table 3. Functional Properties of Acetylcholine (ACh) and CCh Analogues **5a** and **5d** at Human $\alpha_4\beta_2$, $\alpha_3\beta_4$, and α_7 nAChRs Expressed in *Xenopus* Oocytes^a

| | EC ₅₀ (μ M) | pEC ₅₀ [95% CI] | R _{max} [95% CI] (%) |
|-------------------|-----------------------------|----------------------------|--------------------------------|
| ACh | | | |
| $\alpha_4\beta_2$ | 70 | 4.15 [4.35–3.96] | 100 |
| $\alpha_3\beta_4$ | 144 | 3.84 [3.97–3.72] | 100 |
| α_7 | 83 | 4.08 [4.19–3.96] | 100 |
| 5a | | | |
| $\alpha_4\beta_2$ | 7.1 | 5.15 [5.33–4.96] | 66 [61–70] |
| $\alpha_3\beta_4$ | > 320 | < 3.5 | 23 \pm 2.1 (at 320 μ M) |
| α_7 | > 320 | < 3.5 | 0.9 \pm 0.3 (at 320 μ M) |
| 5d | | | |
| $\alpha_4\beta_2$ | 85 | 4.07 [4.60–3.53] | 9.5 [7.3–12] |
| $\alpha_3\beta_4$ | > 320 | < 3.5 | 12 \pm 2.4 (at 320 μ M) |
| α_7 | > 320 | < 3.5 | 0.9 \pm 0.3 (at 320 μ M) |

^a Recordings were made using the two-electrode voltage clamp technique. EC₅₀ values are given in μ M, and pEC₅₀ values are given with 95% confidence intervals in brackets. R_{max} values of **5a** and **5d** at the $\alpha_4\beta_2$ nAChR are given in % of the R_{max} of ACh with 95% confidence intervals in brackets. The responses elicited in oocytes expressing $\alpha_3\beta_4$ and α_7 nAChRs at the maximal concentrations of **5a** and **5d** (320 μ M) are given as % of the R_{max} of ACh.

been incorporated into azetidines ring systems with different substituents (compounds **5a–f**) or a pyrrole ring (compound **5g**). In addition, we explore the SARs of the corresponding series of esters, i.e., the one-carbon analogues of ACh having a methyl group at the C3 carbon (compounds **5h–l**).

Structure–Activity Relationships of the CCh Analogues.

Introduction of an azetidines ring in the CCh analogue resulted in a series of compounds of which several displayed low nanomolar binding affinities to the $\alpha_4\beta_2$ nAChR. In addition, the compounds displayed significant selectivities for the $\alpha_4\beta_2$ subtype, in particular over the $\alpha_3\beta_4$ nAChR but also over the $\alpha_4\beta_4$ nAChR (Table 1 and Figure 3, left). The nonsubstituted azetidines ring analogue **5a** displayed a 2000-fold higher binding affinity to the $\alpha_4\beta_2$ than to the $\alpha_3\beta_4$, and thus, the selectivity profile of **5a** was comparable to that of our original lead, compound **1**.²⁶ Introduction of a methyl group in the 3-position of the azetidines ring yielded compound **5d**, which displayed a K_i value of 2 nM at the $\alpha_4\beta_2$ subtype and a $K_i(\alpha_3\beta_4)/K_i(\alpha_4\beta_2)$ ratio of 11 000, making this compound the ligand with the highest $\alpha_4\beta_2$ binding affinity and the highest $\alpha_4\beta_2/\alpha_3\beta_4$ selectivity in the CCh analogue series to date (Table 1).^{25,26} The presence of two methyl groups or two fluoro atoms in the 3-position of the azetidines ring led to compounds **5b** and **5c**, which displayed significantly decreased binding affinities at all three heteromeric nAChR subtypes compared to **5a** and **5d**, indicating that the presence of an additional substituent in the

3-position of the azetidines ring is not well tolerated in the orthosteric site of the nAChR (Table 1). The 2-dimethylated azetidines ring analogue **5f** exhibited 40-fold lower binding affinity to the $\alpha_4\beta_2$ subtype than **5a**, whereas the binding of **5f** to $\alpha_3\beta_4$ was less impaired by the substitutions in the 2-position. Hence, substituents in the 2-position of the azetidines ring gave rise to compounds with a lower degree of selectivity between the β_2 - and β_4 -containing subtypes.

An additional finding in this study was that azetidines ring analogue **5a** exhibited a significantly increased binding affinity at the $\alpha_4\beta_2$ nAChR compared to the corresponding pyrrolidines and piperidines ring analogues (compounds **3** and **4**, respectively). However, the affinity differences of these three compounds were less pronounced at the β_4 -containing subtypes. Thus, the size of the carbamate containing ring system appears to be a critical determinant of $\alpha_4\beta_2$ binding and β_2/β_4 -selectivity. In order to probe this observation in greater detail, we attempted to synthesize the aziridines analogue of the CCh analogue. Unfortunately, this compound could not be isolated because of its instability. Compound **5g**, where the carbamate nitrogen was incorporated into a pyrrole ring system, displayed weak binding affinities to all three heteromeric nAChRs, which was in good agreement with the low binding affinities of the pyrrolidines analogue **3**. Interestingly, the CCh analogue containing the six-membered piperidines ring system displayed higher binding affinities to all three heteromeric nAChRs than the two compounds with five-membered ring systems (**3** and **5g**), which suggests that factors other than the sheer size of the ring system determine the nAChR binding affinity of these compounds.

Finally, the individual isomers of **5d** ((*R*)-**5d** and (*S*)-**5d**) were synthesized in order to confirm the findings in previous studies of (*R*)-**1**, (*S*)-**1**, (*R*)-**2**, and (*S*)-**2**, where the nAChR activity of the CCh analogues were found to reside primarily in the *R*-enantiomer.²⁵ In concordance with these studies, the *R*-enantiomer of **5d** displayed significantly higher binding affinities (5- to 60-fold) to all three heteromeric nAChRs than (*S*)-**5d**. Since the enantiomeric purity of (*S*)-**5d** was estimated to be >95%, we cannot rule out the possibility that the weaker nAChR binding displayed by the *S*-enantiomer may arise from the presence of trace amounts of (*R*)-**5d** in the (*S*)-**5d** sample. However, the overall conclusion must be that (*R*)-**5d** is the major determinant of the nAChR activity displayed by the racemic compound. In light of this and the results from our previous studies,²⁵ it is reasonable to assume that the same relationship exists for the rest of the compounds in the CCh and ACh series.

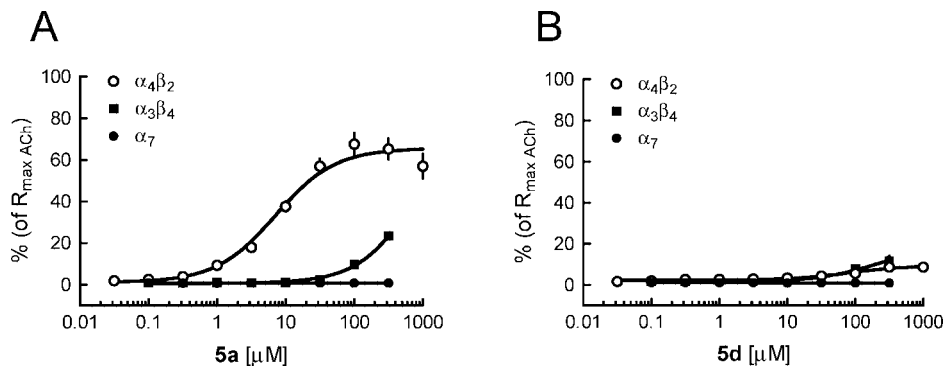


Figure 6. Functional profiles of compounds **5a** (A) and **5d** (B) at human $\alpha_4\beta_2$, $\alpha_3\beta_4$, and α_7 nAChRs expressed in *Xenopus* oocytes. Recordings were made using the two-electrode voltage clamp technique, and data represent the mean \pm SEM from three to five separate experiments.

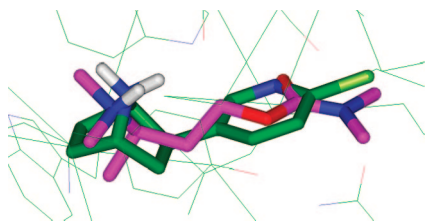


Figure 7. Superimposition of the bound conformation of epibatidine (as determined by X-ray structure)⁶⁶ with a low energy conformation of compound (*R*)-2.

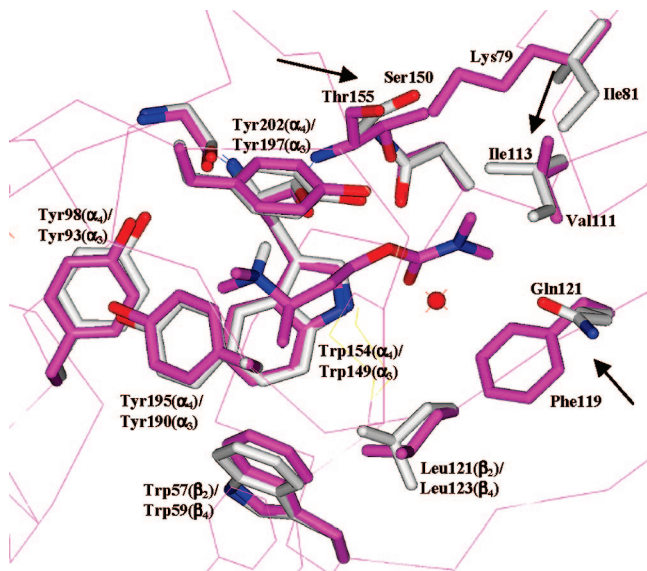


Figure 8. Compound (*R*)-2 docked into the binding site of the $\alpha_4\beta_2$ (shown in purple) and $\alpha_3\beta_4$ receptor (shown in white). The Val111(β_2)/Ile113(β_4), Phe119(β_2)/Gln121(β_4), and Thr155(α_4)/Ser150(α_3) residues likely to have an effect on $\alpha_4\beta_2/\alpha_3\beta_4$ selectivity are marked with an arrow.

Structure–Activity Relationships of the ACh Analogues.

In the ACh analogue series, the cyclopropyl analogue **5j** was the only compound displaying a low nanomolar binding affinity to the $\alpha_4\beta_2$ nAChR similar to those of the CCh analogues **5a** and **5d** (Table 1 and Figure 3). Furthermore, **5j** displayed a 1100-fold lower binding affinity to the $\alpha_3\beta_4$ subtype, thus exhibiting a similar, yet somewhat decreased, selectivity profile as the two CCh analogues. The methyl, isopropyl, and cyclobutyl ACh analogues, **5h**, **5i**, and **5k**, respectively, displayed 10- to 30-fold lower binding affinities to the $\alpha_4\beta_2$ subtype than **5j**, whereas they displayed similar K_i values at the $\alpha_3\beta_4$ and the $\alpha_4\beta_4$ nAChRs. Compounds **5h**, **5i**, and **5k** thus displayed lower

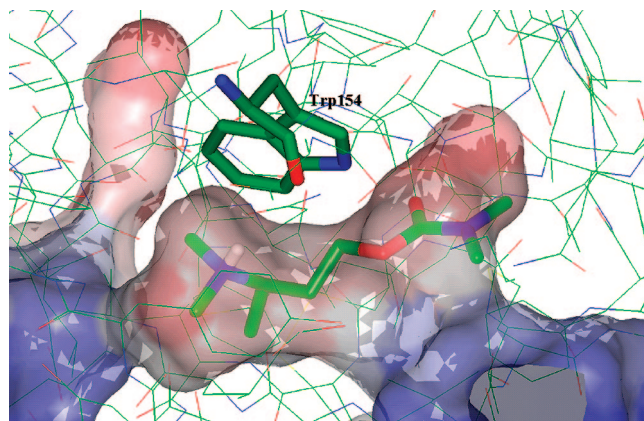


Figure 9. Compound (*R*)-2 docked in the binding pocket of the $\alpha_4\beta_2$ receptor. The displayed PASS⁷⁷ contour shows the cavities in the protein structure. A red color signifies deep burial in the protein, whereas the blue area is closer to the surface.

preference for the $\alpha_4\beta_2$ subtype than **5j** (Table 1). Interestingly, introduction of a phenyl group next to the carbonyl group (compound **5l**) resulted in a dramatically decreased binding affinity to the β_4 -containing nAChR subtypes, and although **5l** displayed the lowest binding affinities at all three heteromeric nAChRs in the series, the compound did exhibit significant preference for the $\alpha_4\beta_2$ over the $\alpha_4\beta_4$ and the $\alpha_3\beta_4$ nAChRs (Table 1).

One might expect that a certain trend would be observed between the corresponding carbamates and esters (i.e., **2** and **5i**, **5a** and **5k**), yet no such overall trend was observed when comparing the binding properties of the respective compounds. However, the bulkiness of the substituents (e.g., an isopropyl being more bulky than a *N,N*-dimethylamino group) is likely to have an effect on receptor binding, but further studies are needed to shed light on this issue.

Binding Modes of CCh and ACh Analogues. The *R*-enantiomers in the series of CCh analogues have higher binding affinities to the nAChRs than the *S*-enantiomers (as seen for (*R*)-**1**, (*S*)-**1**, (*R*)-**2**, (*S*)-**2**,²⁵ (*R*)-**5d**, and (*S*)-**5d**), and thus, the former enantiomers were docked into our homology model. The following considerations and analyses are based on the docked structures, although the pharmacological data are from racemic compounds. Consequently, the assumption is made that the higher $\alpha_4\beta_2$ binding affinity of the *R*- vs the *S*-enantiomer observed for **1**, **2**, and **5d** is consistent throughout the series of CCh and ACh analogues and thus that the nAChR activities of all compounds reside primarily in the *R*-enantiomer.

The lead compounds **1** and **2** display comparable binding to the $\alpha_4\beta_2$ nAChR and yet exhibit significantly different binding

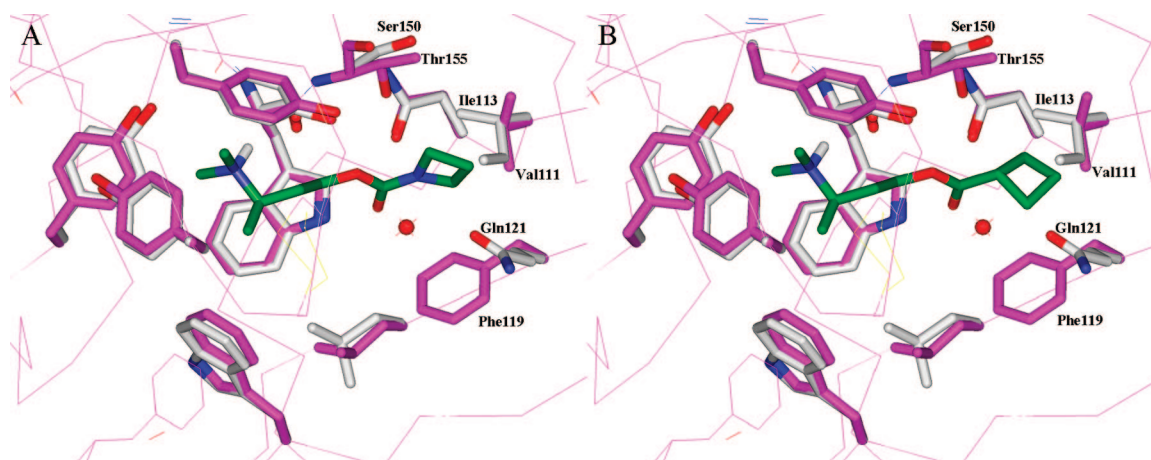


Figure 10. Compound (*R*)-**5a** (A) and compound (*R*)-**5k** (B) docked into the binding site of the $\alpha_4\beta_2$ (shown in purple) and the $\alpha_3\beta_4$ (shown in white) nAChR. Methyl groups in the 3-position of the azetidinium ring of (*R*)-**5a** clash with the Ile113(β_4) residue of the $\alpha_3\beta_4$ nAChR, whereas only the methyl group pointing upward in the 3-position will clash with the Val111(β_2) residue of the $\alpha_4\beta_2$ nAChR. The cyclobutane ring of (*R*)-**5k** is in very close proximity with the Phe119(β_2) residue of the $\alpha_4\beta_2$ nAChR while not displaying this steric clash with the Gln121(β_4) residue of the $\alpha_3\beta_4$ nAChR.

affinities to the β_4 -containing nAChRs. In the *L*-AChBP, the Arg104, Leu112, and Met114 residues form hydrophobic contacts to the carbamate moiety of CCh,⁶⁴ and translated into $\alpha_4\beta_2/\alpha_3\beta_4$ -terminology, these residues correspond to Val111(β_2)/Ile113(β_4), Phe119(β_2)/Gln121(β_4), and Leu121(β_2)/Leu123(β_4), respectively.^{63,69} In addition, homology modeling of the $\alpha_4\beta_2$ and the $\alpha_3\beta_4$ nAChR has assigned Lys79(β_2)/Ile81(β_4) and Phe119(β_2)/Gln121(β_4) to be the major contributors to the difference in topology and electrostatic environment in the binding pocket of the $\alpha_4\beta_2$ and the $\alpha_3\beta_4$ nAChRs.⁶⁹ Taking these considerations into account, it is not surprising that compounds **1** and **2** have different selectivity profiles. The aromatic–amide interaction⁷³ between Phe119 (in the $\alpha_4\beta_2$ nAChR) and the carbamate group of **1** and **2** is nonexistent in the β_4 -containing nAChR because the Phe119(β_2) residue is replaced by Gln121(β_4), which is incapable of such interaction. In return, the loss of the favorable aromatic–amide interaction in the β_4 -containing nAChR can be somewhat outweighed by hydrophobic interactions with residues Ile113(β_4), Leu123(β_4), and Ile81(β_4), which **2** (because of the additional *N*-methyl group) is more able to satisfy than **1** (Figure 8). The importance of ligands complying with the hydrophobic interactions is supported by the fact that CCh binds less efficiently to the nAChR than does MCC (*N*-methylcarbamoylcholine) and DMCC (*N,N*-dimethylcarbamoylcholine), where one or two hydrogens have been replaced by methyl groups.^{26,74–76}

As mentioned above, the Val111(β_2)/Ile113(β_4) and Phe119(β_2)/Gln121(β_4) residues are involved in ligand binding and most likely affect the selectivity of epibatidine, nicotine, and compounds **1** and **2**. It is therefore also plausible that these residues are involved in controlling the selectivities of **5a–i** to the $\alpha_4\beta_2$ over the $\alpha_3\beta_4$ nAChR, and dockings of the CCh and ACh analogues (exemplified by **5a** in Figure 10A and **5k** in Figure 10B) do indicate that these residues are key players when the compounds bind.

Compounds **5a** and **5d** display higher binding affinity to and higher selectivity for the $\alpha_4\beta_2$ nAChR than the parent compound **2**. The increased binding affinity might be explained by the degree of favorable hydrophobic interactions being satisfied upon binding in the receptor binding pocket, as the azetidinium group of **5a** fills out the favorable space in the $\alpha_4\beta_2$ nAChR to a greater extent than does the carbamate *N*-methyl groups of **2**. The greatly enhanced $\alpha_4\beta_2/\alpha_3\beta_4$ selectivity of **5a** and **5d**

compared to **2** is probably explained by the fact that the azetidinium ring has steric clashes with the Ile113(β_4) of the $\alpha_3\beta_4$ nAChR while not having this steric interaction with the Val111(β_2) in the $\alpha_4\beta_2$ nAChR (Figure 10A). Substituting one of the hydrogens in the 3-position of the azetidinium ring with a smaller group like methyl (as in **5d**) enhances the steric interaction with Ile113(β_4) and thus increases the selectivity for the $\alpha_4\beta_2$ nAChR. However, substituting an additional hydrogen in the 3-position (as in **5b** and **5c**) leads to decreased binding and selectivity, as this second group clashes with both receptors.

However, the interaction of the CCh analogues with the Ile113(β_4)/Val111(β_2) residues is not the only factor underlying the $\alpha_4\beta_2/\alpha_3\beta_4$ nAChR selectivity, since differences in binding to the two β_4 -containing nAChRs are also observed (i.e., the binding affinities of **5a–i** to the $\alpha_4\beta_4$ nAChR differ from the binding affinities to the $\alpha_3\beta_4$ nAChR). The dockings of **5a–i** suggest that the Thr155(α_4)/Ser150(α_3) residues are responsible for the observed differences, as they are in close vicinity to the CCh and ACh analogues upon binding. The interaction with Thr155(α_4)/Ser150(α_3) is most pronounced with **5f** where the two methyl groups in the 2-position of the azetidinium ring of the compound extend toward these residues. An additional observation is made when looking at compounds **5e** and **5f**. As compounds **5e** and **5f** are a mixture of rotamers and thus have substituents in the 2- or 4-position of the azetidinium ring, they have steric interactions with Phe119(β_2), which might contribute to their lower binding affinities at the $\alpha_4\beta_2$ nAChR compared to that of **5a**. The decrease in $\alpha_4\beta_2$ binding affinity of **5e** is not as dramatic as for compound **5f**, which is probably ascribed to the fact that **5e** is a mixture of diastereomers. Individual isomers of **5e** thus have a *R* or *S* configuration in the 2 position of the azetidinium ring, and according to the homology model, only the *R* configuration results in steric clashes with Phe119(β_2). The $\alpha_4\beta_2/\alpha_3\beta_4$ selectivity of **5e** and **5f** is lower than those of the other compounds in the **5a–g** series, which could, among other factors, be attributed to the fact that the Ser150(α_3) and Gln121(β_4) residues in the $\alpha_3\beta_4$ nAChR do not enforce steric interactions to the same extent as the corresponding Thr155(α_4) and Phe119(β_2) residues in the $\alpha_4\beta_2$ nAChR.

As mentioned, compound **5e** is a mixture of diastereomers, each of which can exist in two rotameric states as mentioned above. The binding mode analysis for **5e** is therefore very complex, and we will refrain from speculating on this matter

based on the pharmacological data presently available. It is highly likely that one of the isomers of **5e** will be superior to the others in binding to the nAChRs, but the individual isomers of **5e** need to be resolved in order to address this issue in more detail.

The binding properties displayed by the ACh analogues **5h–l** at the $\alpha_4\beta_2$ nAChR are comparable with those of the CCh analogues, and yet the esters exhibit much lower degrees of $\alpha_4\beta_2/\alpha_3\beta_4$ selectivity. The selectivity differences can once again be explained by the Val111(β_2) and Ile113(β_4) residues. In contrast to the azetidine rings in the CCh analogue series, the acyl substituents of the ACh analogues do not quite reach this volume in the receptor models (Figure 10B). Hence, the contribution of the Val111(β_2)/Ile113(β_4) residues to the binding of compounds **5h–l** to the nAChRs is considerably smaller than that to the binding of compounds **5a–f**, and consequently, the $\alpha_4\beta_2/\alpha_3\beta_4$ selectivity of **5h–l** is decreased.

A significant difference in binding affinity is observed between ACh analogue **5k** and the CCh analogue **5a**. The sp^3 -hybridized nature of the acyl carbon atom in **5k** forces the cyclobutane ring to accommodate a different orientation compared to the azetidine ring in **5a**, where the carbamate nitrogen is sp^2 -hybridized. The orientation of the cyclobutane ring results in steric interactions with the Phe119(β_2) residue of the $\alpha_4\beta_2$ nAChR (Figure 10B), and this clash might explain the 20-fold difference in $\alpha_4\beta_2$ binding affinities observed between **5a** and **5k** (Table 1). The ACh analogue **5j**, on the other hand, binds tightly to the receptor because the smaller size of the cyclopropyl group prevents it from clashing with the Phe119(β_2) in the $\alpha_4\beta_2$ nAChR.

Functional Properties of the CCh and ACh Analogues at the nAChRs. The synthesized carbamates and esters were all agonists at the $\alpha_3\beta_4$ nAChR in the FMP assay (Figure 5 and Table 2), just like all other previously synthesized CCh analogues,^{25,26} and the observed agonist potencies correlate well with the corresponding binding affinities at the $\alpha_3\beta_4$ receptor (Figure 5C). In addition, the functional properties of **5a** and **5d** at the three major human neuronal nAChR subtypes $\alpha_4\beta_2$, $\alpha_3\beta_4$, and α_7 (expressed in *Xenopus oocytes*) were characterized in a conventional electrophysiological setup. The high degree of $\alpha_4\beta_2/\alpha_3\beta_4$ selectivity displayed by several of the compounds in this study as well as by previously reported CCh analogues^{25,26} in the [³H]epibatidine binding assay was promising, and consequently, we wanted to investigate whether this binding selectivity translated into functional selectivity. In the TEVC assay, compound **5a** was a functionally selective partial agonist at the $\alpha_4\beta_2$ nAChR, exhibiting only weak agonism at the $\alpha_3\beta_4$ subtype and no activity at the α_7 nAChR. However, it should be stressed that the functional properties of the compound was not determined at the plethora of minor neuronal nAChR subtypes, such as $\alpha_3\beta_2$, $\alpha_4\beta_4$, and others, or at the muscle-type nAChR. Thus, additional functional testing at these nAChRs is required to establish whether **5a** is a completely selective $\alpha_4\beta_2$ nAChR agonist.

Considering the close structural similarity of compounds **5a** and **5d**, the functional profiles of the compounds were remarkably different. In the [³H]epibatidine binding assays, compound **5d** displayed a higher $\alpha_4\beta_2/\alpha_3\beta_4$ selectivity than **5a** (Table 1). However, whereas **5d**, similarly to **5a**, exhibited negligible activities at the $\alpha_3\beta_4$ and α_7 nAChRs, **5d** was a significantly weaker agonist with a dramatically reduced efficacy at the $\alpha_4\beta_2$ nAChR compared to **5a** (Figure 6, Table 3). Thus, the introduction of a methyl group in the 3-position of the azetidine ring in **5a** led to a slightly higher binding affinity to $\alpha_4\beta_2$,

whereas the ring substitution decreased both potency and efficacy of the agonist at this receptor. The high binding affinity and low functional efficacy displayed by **5d** at $\alpha_4\beta_2$ are reminiscent of the pharmacological characteristics of the standard nAChR ligand ABT-089, which displays low-nanomolar K_i values in binding assays to native and recombinant $\alpha_4\beta_2$ receptors and extremely low efficacies at the receptor in functional assays.⁷⁷ Several other examples of divergences between the binding affinities and functional properties displayed by nAChR ligands can be found in the literature.²

The number of truly functionally selective $\alpha_4\beta_2$ nAChR agonists (or more precisely, as the present study allows us to conclude for **5a**, agonists completely functionally selective for $\alpha_4\beta_2$ over $\alpha_3\beta_4$ and α_7 nAChRs) published to this date is not overwhelming.² Compound **5a** displays a more than 40-fold higher potency at the $\alpha_4\beta_2$ nAChR than at the other two major neuronal nAChRs, and in this respect, the compound is comparable to truly $\alpha_4\beta_2$ selective agonists like TC-2559.⁷⁸ In recent years, there has been an increasing interest in the development of partial $\alpha_4\beta_2$ nAChR agonists, in particular following the marketing of the partial $\alpha_4\beta_2$ agonist cytisine (in Eastern Europe, trade name Tabex) and its derivative varenicline (in the U.S. as CHANTIX, in the EU as CHAMPIX) as smoking cessation aids. Partial $\alpha_4\beta_2$ nAChR agonists have been proposed to exert a dual effect beneficial for this indication: a reduction of the craving connected with quitting (due to activation of $\alpha_4\beta_2^*$ heteroreceptors mediating dopamine release in the mesolimbic system) and an inhibition of the nicotine reinforcement when smoking (also mediated predominantly by $\alpha_4\beta_2^*$ receptors).⁷⁹ However, in contrast to compounds **5a** and **5d** from the present study, both cytisine and varenicline, in addition to their partial agonism at $\alpha_4\beta_2$ nAChRs, are characterized by being highly efficacious at several other neuronal nAChR subtypes, including $\alpha_3\beta_4$ and α_7 .^{13,80,81} It would be interesting to evaluate the therapeutic prospects of compound **5a** and other $\alpha_4\beta_2$ selective partial agonists from the CCh and ACh series in models for smoking cessation and for some of the neurodegenerative and psychiatric indications where $\alpha_4\beta_2$ nAChR agonists have been proposed to be potentially beneficial.

Conclusion

In conclusion, the series of carbamates (**5a–g**) presented in this study provides further insight into the SARs of the CCh analogues as nAChR agonists. The observed results combined with our modeling studies present valuable information on how these compounds may bind to the nAChR and identify the receptor residues Val111(β_2)/Ile113(β_4), Phe119(β_2)/Gln121(β_4), and Thr155(α_4)/Ser150(α_3) as possible determinants of the observed $\alpha_4\beta_2/\alpha_3\beta_4$ selectivity exhibited by the compounds. The incorporation of an azetidine ring in the CCh analogue optimizes the receptor–ligand interactions at the $\alpha_4\beta_2$ nAChR, and in agreement with previous observations,²⁵ the nAChR activity of CCh analogue **5d** was observed to reside primarily in the *R*-enantiomer. Hence, it is very likely that this relationship of enantiomeric activity exists for all compounds in the CCh and ACh series. Most importantly, we found that the significant selectivity for the major neuronal $\alpha_4\beta_2$ nAChR subtype displayed by some of the CCh analogues in the binding assays is mirrored in their functional profiles, at least in the case of **5a**, which is a fairly potent agonist at the $\alpha_4\beta_2$ nAChR that has no or limited activity at the $\alpha_3\beta_4$ and α_7 nAChRs. Although not all CCh analogues that display distinct selectivity for the $\alpha_4\beta_2$ in binding assays may be functionally selective as well, as exemplified by **5d**, it is reasonable to assume that the CCh

analogue series synthesized in this and previous studies²⁵ contain additional functionally selective $\alpha_4\beta_2$ agonists.

In addition to the CCh analogues, we report the synthesis and pharmacological characterization of a corresponding series of ACh analogues. While a couple of these analogues display high-affinity binding to the nAChRs, these generally do not display the same degree of $\alpha_4\beta_2/\alpha_3\beta_4$ receptor selectivity as the carbamate compounds in the binding assays. This underlines the importance of having a planar shape around the carbonyl group in the molecule for optimal binding to the nAChRs. However, the effects of atom hybridization need to be analyzed further in order to fully understand the molecular basis underlying the different binding properties of the ACh and the CCh analogues.

Experimental Section

Chemistry. General Procedures. All reactions involving air sensitive reagents were performed under a N₂ atmosphere using syringe–septum cap techniques. Unless otherwise noted, all materials were obtained from commercial suppliers and used without further purification. When dry solvents were used, THF was distilled and stored over molecular sieves (4 Å). All other solvents, stated dry, were purchased from a commercial source and stored over molecular sieves (4 Å). ¹H NMR and ¹³C NMR spectra were obtained on a Varian Gemini 2000 (300 MHz) or Varian Mercury Plus (300 MHz). Flash column chromatography (FC) was performed using Merck silica gel 60 (0.040–0.063 mm). Dry column vacuum chromatography (DCVC) was performed using Merck silica gel 60 (0.015–0.040 mm). Analytical thin-layer chromatography (TLC) was carried out using Merck silica gel 60 F₂₅₄ plates, and the compounds were visualized using KMnO₄ spraying reagent. Elemental analyses were performed at the Analytical Research Department, H. Lundbeck A/S, Denmark, or by J. Theiner, Department of Physical Chemistry, University of Vienna, Austria, and are within $\pm 0.4\%$ of the calculated values unless otherwise stated. Melting points were determined in open capillary tubes and are uncorrected.

(*R*)-3-(Dimethylamino)butan-1-ol ((*R*)-7).^{25,82} A stirred solution of (*R*)-3-aminobutan-1-ol (2.96 g, 33.2 mmol) in MeOH (125 mL) was added to formaldehyde (37% in H₂O, 13.5 mL, 166 mmol) and NaBH(OAc)₃ (35.2 g, 166 mmol). Stirring was continued at room temperature overnight, and NaOH (2 M, 250 mL) was added. The mixture was extracted with CH₂Cl₂, dried (MgSO₄), and evaporated. Purification by DCVC (eluent CH₂Cl₂/NH₄OH/MeOH, 100:0:0 \rightarrow 100:2:18) afforded 2.33 g (60%) of (*R*)-7 as a clear oil. The NMR data of (*R*)-7 were in concordance with the NMR data given in the literature.

(*S*)-3-(Dimethylamino)butan-1-ol ((*S*)-7).²⁵ (*S*)-7 was prepared as described for (*R*)-7 starting from (*S*)-3-aminobutan-1-ol (3.11 g, 34.9 mmol). Yield: 2.55 g (63%). The product was a clear oil. The NMR data of (*S*)-7 were equal to the NMR data of (*R*)-7.

3-Amino-3-methylbutan-1-ol (8).⁸³ To a suspension of 3-amino-3-methylbutanoic acid (10.0 g, 85.4 mmol) in dry THF (50 mL), stirred under nitrogen, was added BF₃OEt₂ (10.8 mL, 85.4 mmol) during 30 min. The resulting mixture was stirred at reflux for 3 h, and BH₃·SMe₂ (90% in MeSH, 10.0 mL, 94.8 mmol) was added slowly. The mixture was stirred at reflux for an additional 5 h, and an additional portion of BH₃·SMe₂ (90% in MeSH, 1.00 mL, 9.48 mmol) was added. Stirring was continued for 1 h. The reaction mixture was cooled to room temperature and quenched by slow addition of a 1:1 THF/H₂O mixture (12 mL) followed by aqueous NaOH (5 M, 71 mL). The resulting two-phase mixture was heated to reflux for 15 h, cooled to room temperature, and filtered. The residual solid was then washed with THF (50 mL \times 3). Evaporation of the combined filtrates gave a slurry, which was extracted with CH₂Cl₂ (100 mL \times 3), dried (MgSO₄), and evaporated to give the product as a yellow oil (8.36 g, 99.8%). The NMR data of **8** were in concordance with the NMR data given in the literature.⁸³

3-Amino-2-methylpropan-1-ol (9).⁸⁴ **9** was prepared as described for **8** from 3-amino-2-methylpropanoic acid (10.0 g, 97.0 mmol), affording **9** as a colorless oil (9.0 g, 105%), which was used without further purification. The NMR data of **9** were in concordance with the NMR data found in the literature.⁸⁴

2-Methyl-3-(4-methylphenylsulfonamido)propyl 4-Methylbenzenesulfonate (10). 3-Amino-2-methylpropan-1-ol (**9**) (5.00 g, 56.1 mmol) was dissolved in pyridine (80 mL) and cooled to 0 °C. *p*-Toluenesulfonyl chloride (19.83 g, 104 mmol) was added slowly, keeping the temperature below 6 °C. After addition, the solution was kept at 4 °C overnight (\sim 19 h), and the mixture was then poured into ice–water (350 mL). The precipitated pyridinium chloride was washed with pyridine, and the pyridine layers were added to the ice–water mixture. A red oil separated, which was isolated, affording 12.70 g of crude **10**. The pyridine–water layer was extracted with CH₂Cl₂, which was then dried (MgSO₄) and evaporated to give a second crop of crude **10** (3.75 g). Crude **10** was dissolved in CHCl₃ and washed with H₂O to remove residual pyridine. Drying (MgSO₄) and evaporation of the chloroform layers then gave **10** (11.6 g, 57%). ¹H NMR (CDCl₃): δ 0.88 (3H, d, *J* = 6.9 Hz), 1.95–2.05 (1H, m), 2.42 (3H, s), 2.45 (3H, s), 2.83 (1H, t, *J* = 6.7 Hz), 3.85 (1H, dd, *J* = 5.7/10.0 Hz), 3.95 (1H, dd, *J* = 4.9/9.9 Hz), 5.07 (1H, t, *J* = 6.7 Hz), 7.28 (2H, d, *J* = 8.0 Hz), 7.33 (2H, d, *J* = 8.0 Hz), 7.69 (2H, d, *J* = 8.2 Hz), 7.74 (2H, d, *J* = 8.2 Hz). ¹³C NMR (CDCl₃): δ 14.28, 21.66, 21.80, 33.66, 45.11, 72.15, 127.07, 127.96, 129.87, 130.06, 132.59, 136.83, 143.56, 145.16.

3-Methyl-3-(4-methylphenylsulfonamido)butyl 4-Methylbenzenesulfonate (13). **13** was prepared as described for **10** from 3-amino-3-methylbutan-1-ol (**8**) (4.00 g, 38.8 mmol) to give **13** as a red oil (5.18 g, 84%). No further purification was performed. ¹H NMR (CDCl₃): δ 1.15 (6H, s), 1.94 (2H, t, *J* = 6.3 Hz), 2.42 (6H, s), 4.12 (2H, t, *J* = 6.3 Hz), 4.79 (1H, NH), 7.24–7.35 (4H, m), 7.69–7.77 (4H, m).

3-Methyl-1-tosylazetidide (10a). To a solution of *t*-BuOK (1.41 g, 12.6 mmol) in *t*-BuOH (200 mL) was added 2-methyl-3-(4-methylphenylsulfonamido)propyl 4-methylbenzenesulfonate (**10**) (5.00 g, 12.6 mmol). The reaction mixture was heated to reflux overnight, cooled to room temperature, filtered, and evaporated. The crude product was dissolved in MeOH and precipitated with H₂O. This afforded **10a** (2.49 g, 88%) as a brown/black hard wax. ¹H NMR (CDCl₃): δ 1.02 (3H, d, *J* = 6.8 Hz), 2.43–2.56 (1H, m), 2.46 (3H, s), 3.31 (1H, d, *J* = 6.2 Hz), 3.34 (1H, d, *J* = 6.1 Hz), 3.85 (1H, d, *J* = 8.1 Hz), 3.87 (1H, d, *J* = 8.1 Hz), 7.36 (2H, d, *J* = 7.9 Hz), 7.71 (2H, d, *J* = 8.2 Hz). ¹³C NMR (CDCl₃): δ 19.05, 21.76, 23.74, 57.57, 128.49, 129.77, 131.68, 143.98.

2,2-Dimethyl-1-tosylazetidide (13a). **13a** was prepared as described for **10a** from 3-methyl-3-(4-methylphenylsulfonamido)butyl 4-methylbenzenesulfonate (**13**) (5.94 g, 14.4 mmol). The crude product was dissolved in MeOH and precipitated with H₂O. Two consecutive recrystallizations from MeOH–H₂O afforded 1.67 g (49%) of **13a** as yellow crystals. The mother liquor was evaporated and the crystals thus obtained were recrystallized from MeOH–H₂O, giving 549 mg (16%) of yellow crystals. Mp: 95.1–95.8 °C. ¹H NMR (CDCl₃): δ 1.45 (6H, s), 1.98 (2H, t, *J* = 7.5 Hz), 2.42 (3H, s), 3.71 (2H, t, *J* = 7.5 Hz), 7.27 (2H, d, *J* = 8.3 Hz), 7.70 (2H, d, *J* = 8.3 Hz). ¹³C NMR (CDCl₃): δ 21.96, 28.11, 31.50, 45.60, 71.79, 127.96, 129.84, 137.39, 143.46. Anal. (C₁₂H₁₇NO₂S) C, H, N.

3-Methylazetidinium Hydrochloride (10b). To a solution of 3-methyl-1-tosylazetidide (**10a**) (2.49 g, 11.1 mmol) in *n*-pentanol (60 mL) was added Na (5.08 g, 221 mmol) in small pieces. After being stirred at reflux overnight, the solution was cooled and H₂O (75 mL) added. The organic layer was separated and extracted with aqueous HCl (2 M, 2 \times 100 mL). Evaporation of the aqueous layer gave 1.07 g (90%) of **10b** as a brown wet crystalline compound. ¹H NMR (D₂O): δ 1.09 (3H, d, *J* = 6.9 Hz), 2.83–2.96 (1H, m), 3.61 (2H, t, *J* = 9.1 Hz), 4.00 (2H, t, 9.6 Hz). ¹³C NMR (D₂O): δ 18.25, 27.68, 53.53.

2,2-Dimethylazetidinium Hydrochloride (13b). **13b** was prepared described for **10b** from 2,2-dimethyl-1-tosylazetidide (**13a**) (2.20

g, 9.19 mmol). The product **13b** was isolated as wet yellow crystals (1.57 g). The crude product was used without further purification. $^1\text{H NMR}$ (D_2O): δ 1.51 (6H, s), 2.29 (2H, t, $J = 8.5$ Hz), 3.81 (2H, t, $J = 8.5$ Hz). $^{13}\text{C NMR}$ (D_2O): δ 26.67, 31.96, 39.81, 68.64.

3-((Azetidine-1-carboxyloxy)-1-methylpropyl)dimethylammonium Oxalate (5a). To a solution of 3-(dimethylamino)butan-1-ol (200 mg, 1.71 mmol) in dry toluene (5 mL) was added CDI (332 mg, 2.05 mmol). The mixture was stirred for 3 h at room temperature, and dry THF (2 mL) was added. The solution was further stirred for 1 h, and azetidine (0.23 mL, 3.4 mmol) was added. The resultant mixture was stirred overnight (18 h), EtOAc (10 mL) was added, and the mixture was washed with brine (10 mL). The organic phase was dried (MgSO_4), evaporated, and purified by DCVC (eluent $\text{CH}_2\text{Cl}_2/\text{NH}_4\text{OH}/\text{MeOH}$, 100:0:0 \rightarrow 200:2:30). This gave 199 mg (58%) of **5a** as the free amine. The product was a colorless oil. The free amine of **5a** (149 mg, 0.743 mmol) was added to a solution of oxalic acid (74 mg, 0.82 mmol) in dry $^i\text{Pr-OH}$ (1 mL), and the mixture was stored at 4 $^\circ\text{C}$ until crystallization. Filtration and recrystallization ($^i\text{Pr-OH}$, Et_2O) gave 175 mg (81%) of **5a** as colorless crystals. Mp: 112–113 $^\circ\text{C}$. $^1\text{H NMR}$ (D_2O): δ 1.13 (3H, d, $J = 6.5$ Hz), 1.64–1.75 (1H, m), 1.88–1.97 (1H, m), 1.99–2.10 (2H, m), 2.59 (3H, s), 2.63 (3H, s), 3.26–3.37 (1H, m), 3.81 (4H, t, $J = 7.4$ Hz) 3.89–4.03 (2H, m). $^{13}\text{C NMR}$ (D_2O): δ 13.13, 15.81, 30.55, 38.47, 40.37, 49.92, 60.10, 62.26, 158.12, 166.13. Anal. ($\text{C}_{12}\text{H}_{22}\text{N}_2\text{O}_6$) C, H, N.

3-((3,3-Dimethylazetidine-1-carboxyloxy)-1-methylpropyl)dimethylammonium Oxalate (5b). **5b** was prepared as described for **5a** from 3-(dimethylamino)butan-1-ol (**7**) (200 mg, 1.71 mmol) and 3,3-dimethylazetidine (291 mg, 3.41 mmol). The free amine of **5b** was isolated as a colorless oil (201 mg, 52%). The free amine of **5b** (100 mg, 0.44 mmol) was added to a solution of oxalic acid (43 mg, 0.48 mmol) in a few drops of distilled acetone, and the mixture was stored at 4 $^\circ\text{C}$ until crystallization. Filtration gave 53 mg (38%) of **5b** as colorless crystals. Evaporation of the filtrate and addition of acetone precipitated an additional 19 mg (14%) of **5b**. Mp: 99–100 $^\circ\text{C}$. $^1\text{H NMR}$ (D_2O): δ 1.05 (6H, s), 1.16 (3H, d, $J = 6.7$ Hz), 1.66–1.78 (1H, m), 1.90–1.99 (1H, m), 2.61 (3H, s), 2.65 (3H, s) 3.25–3.38 (1H, m), 3.51 (4H, s), 3.88–4.05 (2H, m). $^{13}\text{C NMR}$ (D_2O): δ 13.19, 26.44, 30.51, 30.86, 31.42, 38.52, 40.31, 60.18, 61.90, 62.34, 158.52, 166.39. Anal. ($\text{C}_{14}\text{H}_{26}\text{N}_2\text{O}_6 \cdot 1 \text{ H}_2\text{O}$) C, H, N.

3-((3,3-Difluoroazetidine-1-carboxyloxy)-1-methylpropyl)dimethylammonium Oxalate (5c). To a solution of 3-(dimethylamino)butan-1-ol (**7**) (300 mg, 2.56 mmol) in dry toluene (7.5 mL) was added CDI (498 g, 3.07 mmol). The mixture was stirred for 3 h at room temperature, and dry THF (3 mL) was added. The solution was further stirred for 1 h, and a solution of 3,3-difluoroazetidinium hydrochloride (497 mg, 3.83 mmol) in aqueous NaOH (2 M, 2 mL) was added. The resultant mixture was stirred overnight. The organic layer was separated, and the aqueous layer was extracted with toluene (4 \times 10 mL). The combined organic phases were dried (MgSO_4), filtered, and evaporated, affording the free amine of **5c** (366 mg, 61%). The product was a yellow oil. The oxalate salt (**5c**) was prepared as described for **5b** from oxalic acid (42 mg, 0.47 mmol) and the free amine of **5c** (100 mg, 0.42 mmol). The product was isolated as colorless crystals (112 mg, 82%). Mp: 115.8–116.6 $^\circ\text{C}$. $^1\text{H NMR}$ (D_2O): δ 1.33 (3H, d, $J = 6.7$ Hz), 1.85–1.96 (1H, m), 2.09–2.20 (1H, m), 2.78 (3H, s), 2.81 (3H, s), 3.45–3.56 (1H, m), 4.10–4.27 (2H, m), 4.39 (4H, t, $J = 12.2$ Hz). $^{13}\text{C NMR}$ (D_2O): δ 13.12, 30.38, 38.52, 40.31, 59.99, 61.58 (t, $J = 28.8$ Hz), 62.99, 115.96 (t, $J = 272$ Hz), 158.10, 166.27. Anal. ($\text{C}_{12}\text{H}_{20}\text{F}_2\text{N}_2\text{O}_6$) C, H, N.

3-((3-Methylazetidine-1-carboxyloxy)-1-methylpropyl)dimethylammonium Oxalate (5d). **5d** was prepared as described for **5c** from 3-(dimethylamino)butan-1-ol (**7**) (300 mg, 2.56 mmol) and 3-methylazetidinium hydrochloride (**10b**) (551 mg, 5.11 mmol). However, purification was performed by FC (Et_2O , MeOH, NH_3 , 10:100:1 \rightarrow 20:100:1), affording 362 mg (66%) of the free amine of **5d** as a colorless oil. The oxalate salt **5d** was prepared as described for **5b** from oxalic acid (46 mg, 0.51 mmol) and the free amine of **5d** (100 mg, 0.47 mmol). The product was isolated as colorless

crystals (84.2 mg, 60%). Mp: 92.2–92.8 $^\circ\text{C}$. $^1\text{H NMR}$ (D_2O): δ 1.17 (3H, d, $J = 6.9$ Hz), 1.32 (3H, d, $J = 6.6$ Hz), 1.82–1.93 (1H, m), 2.06–2.16 (1H, m), 2.63–2.72 (1H, m), 2.77 (3H, s), 2.81 (3H, s), 3.43–3.57 (3H, m), 4.03–4.21 (4H, m). $^{13}\text{C NMR}$ (D_2O): δ 13.18, 19.28, 24.43, 30.53, 38.52, 40.34, 56.45, 60.15, 62.29, 158.28, 166.19. Anal. ($\text{C}_{13}\text{H}_{24}\text{N}_2\text{O}_6 \cdot \frac{1}{3}\text{H}_2\text{O}$).

(R)-3-((3-Methylazetidine-1-carboxyloxy)-1-methylpropyl)dimethylammonium Oxalate (R-5d). (*R*)-**5d** was prepared as described for **5d** starting from (*R*)-3-(dimethylamino)butan-1-ol (**7**) (400 mg, 3.41 mmol). The product was isolated as colorless crystals. Overall yield starting from (*R*)-(**7**) was 8.6%, >95% ee. Mp: 84.3–84.5 $^\circ\text{C}$. NMR data were as seen for **5d**. Anal. ($\text{C}_{13}\text{H}_{24}\text{N}_2\text{O}_6 \cdot \frac{1}{3}\text{H}_2\text{O}$).

(S)-3-((3-Methylazetidine-1-carboxyloxy)-1-methylpropyl)dimethylammonium Oxalate (S-5d). (*S*)-**5d** was prepared as described for **5d** starting from (*S*)-3-(dimethylamino)butan-1-ol (**7**) (400 mg, 3.41 mmol). The product was isolated as colorless crystals. Overall yield starting from (*S*)-(**7**) was 10%, >95% ee. Mp: 96.7–96.8 $^\circ\text{C}$. NMR data were as seen for **5d**. Anal. ($\text{C}_{13}\text{H}_{24}\text{N}_2\text{O}_6$).

3-((2-Methylazetidine-1-carboxyloxy)-1-methylpropyl)dimethylammonium Oxalate (5e). **5e** was prepared as described for **5c** from 3-(dimethylamino)butan-1-ol (**7**) (300 mg, 2.56 mmol) and 2-methylazetidinium hydrochloride (522 mg, 4.85 mmol). However, purification was performed by FC (Et_2O , MeOH, NH_3 , 10:100:1 \rightarrow 20:100:1), affording 462 mg (84%) of **5e** (as the free amine). The product was a colorless oil. The oxalate salt **5e** was prepared as described for **5b** from oxalic acid (46 mg, 0.51 mmol) and the free amine of **5d** (100 mg, 0.47 mmol). The product was isolated as colorless crystals (106 mg, 74%). An analytical portion was recrystallized from CH_2Cl_2 – Et_2O . Mp: 76.4–77.1 $^\circ\text{C}$. $^1\text{H NMR}$ (D_2O): δ 1.32 (3H, d, $J = 6.7$ Hz), 1.34 (3H, d, $J = 6.4$ Hz), 1.78–1.93 (2H, m), 2.05–2.16 (1H, m), 2.30–2.42 (1H, m), 2.77 (3H, s), 2.80 (3H, s), 3.40–3.53 (1H, m), 3.84–3.90 (2H, m), 4.03–4.21 (2H, m), 4.31–4.42 (1H, m). $^{13}\text{C NMR}$ (D_2O): δ 13.23, 20.96, 23.93, 30.46, 38.61, 40.20, 46.86, 59.18, 60.13, 62.02, 158.16, 166.27. Anal. ($\text{C}_{13}\text{H}_{24}\text{N}_2\text{O}_6$) C, H, N.

3-((2,2-Dimethylazetidine-1-carboxyloxy)-1-methylpropyl)dimethylammonium Oxalate (5f). **5f** was prepared as described for **5c** from 3-(dimethylamino)butan-1-ol (**7**) (300 mg, 2.56 mmol) and 2,2-dimethylazetidinium hydrochloride (**13b**) (~5 mmol). However, purification was performed by FC (Et_2O , MeOH, NH_3 , 10:100:1 \rightarrow 15:100:1) followed by DCVC ($\text{CH}_2\text{Cl}_2/\text{MeOH}/\text{NH}_3$, 100:10:1), affording 185 mg (32%) of **5f** (as the free amine). The product was a yellow oil. The oxalate salt **5f** was prepared as described for **5b** from oxalic acid (34 mg, 0.38 mmol) and the free amine of **5f** (79 mg, 0.35 mmol). The product was isolated as colorless crystals (88.3 mg, 80%). An analytical portion was recrystallized from CH_2Cl_2 – Et_2O . Mp: 93.3–94.2 $^\circ\text{C}$. $^1\text{H NMR}$ (D_2O): δ 1.19–1.22 (3H, m), 1.29 (6H, s), 1.69–1.80 (1H, m), 1.93 (2H, t, $J = 7.8$ Hz), 1.93–2.08 (1H, m), 2.65 (3H, s), 2.68 (3H, s), 3.29–3.39 (1H, m), 3.62–3.76 (2H, m), 3.90–4.12 (2H, m). $^{13}\text{C NMR}$ (D_2O): δ 13.15, 28.37, 30.51, 37.24, 38.54, 40.32, 42.48, 60.18, 61.93, 71.21, 158.71, 165.77. Anal. ($\text{C}_{14}\text{H}_{26}\text{N}_2\text{O}_6$) C, H, N.

3-((1H-Pyrrole-1-carboxyloxy)-1-methylpropyl)dimethylammonium Oxalate (5g). 1-[3-(Dimethylamino)propyl]-3-ethylcarbodiimide hydrochloride (EDC \cdot HCl) (1.14 g, 5.95 mmol) was added to a solution of pyrrole-1-carboxylic acid (700 mg, 6.30 mmol) in dry CH_2Cl_2 (21 mL) at room temperature, and the mixture was allowed to stir at room temperature for 15 min. The sodium salt of **7** (generated in dry THF (14 mL) from **7** (369 mg, 3.15 mmol) and NaH (60% dispersion on mineral oil, 126 mg, 3.15 mmol)) was added, and the resulting mixture was stirred at room temperature for 1 h. Filtration, evaporation, and DCVC (CH_2Cl_2 , MeOH, NH_3 , 100% \rightarrow 100:2.5:0.5) yielded 214 mg (32%) of **5g** (as the free amine). The product was a colorless oil. The oxalate salt **5g** was prepared as described for **5b** from oxalic acid (20 mg, 0.22 mmol) and the free amine of **5g** (42 mg, 0.20 mmol). The product was isolated as colorless crystals (49.5 mg, 83%). An analytical portion was recrystallized from CH_2Cl_2 – Et_2O . Mp: 122–123 $^\circ\text{C}$. $^1\text{H NMR}$ (D_2O): δ 1.38 (3H, d, $J = 6.7$ Hz), 1.98–2.10 (1H, m), 2.25–2.36 (1H, m), 2.81 (3H, s), 2.84 (3H, s), 3.55–3.64 (1H, m), 4.39–4.56 (2H, m), 6.31–6.33 (2H, m), 7.27–7.31 (2H, m).

^{13}C NMR (D_2O): δ 13.11, 30.09, 38.59, 40.24, 59.92, 64.44, 113.58, 120.98, 151.92, 166.47. Anal. ($\text{C}_{13}\text{H}_{20}\text{N}_2\text{O}_6$) C, H, N.

3-((Acetoxy)-1-methylpropyl)dimethylammonium Oxalate (5h). 3-(Dimethylamino)butan-1-ol (300 mg, 2.56 mmol) was dissolved in dry CH_2Cl_2 (12 mL) and cooled to 0 °C. Acetyl chloride (0.20 mL, 2.8 mmol) was added slowly, and the mixture was stirred at room temperature for 5 h. The solvent was evaporated, and the residue was dissolved in CH_2Cl_2 (10 mL) and washed with cold aqueous NaOH (1 M, 5 mL). The organic phase was dried (MgSO_4), evaporated, and purified by DCVC ($\text{CH}_2\text{Cl}_2/\text{MeOH}$, 100 \rightarrow 100:6), affording 341 mg (84%) of **5h** (as the free amine). The product was a colorless oil. The oxalate salt **5h** was prepared as described for **5b** from oxalic acid (62 mg, 0.69 mmol) and the free amine of **5h** (100 mg, 0.63 mmol). The product was isolated as colorless crystals (90.6 mg, 61%). An analytical portion was recrystallized twice from $\text{CH}_2\text{Cl}_2\text{-Et}_2\text{O}$. Mp: 106.9–107.6 °C. ^1H NMR (D_2O): δ 1.16 (3H, d, $J = 6.7$ Hz), 1.69–1.80 (1H, m), 1.92 (3H, s), 1.92–2.04 (1H, m), 2.62 (3H, s), 2.66 (3H, s), 3.31–3.42 (1H, m), 3.92–4.00 (1H, m), 4.04–4.11 (1H, m). ^{13}C NMR (D_2O): δ 12.97, 20.21, 30.02, 38.47, 40.40, 60.01, 61.82, 165.65, 174.79. Anal. ($\text{C}_{10}\text{H}_{19}\text{NO}_6$) C, H, N.

3-((Isobutyryloxy)-1-methylpropyl)dimethylammonium Oxalate (5i). **5i** was prepared as described for **5h** from 3-(dimethylamino)butan-1-ol (**7**) (300 mg, 2.56 mmol) and isobutyryl chloride (0.29 mL, 2.8 mmol). The amino ester **5i** was isolated as the free amine (384 mg, 80%). The product was a colorless oil. The oxalate salt **5i** was prepared as described for **5b** from oxalic acid (53 mg, 0.59 mmol) and the free amine of **5i** (100 mg, 0.53 mmol). The product was isolated as colorless crystals (90.6 mg, 61%). An analytical portion was recrystallized from $\text{CH}_2\text{Cl}_2\text{-Et}_2\text{O}$. Mp: 107.4–108.3 °C. ^1H NMR (D_2O): δ 1.12 (6H, d, $J = 7.0$ Hz), 1.33 (3H, d, $J = 6.7$ Hz), 1.85–1.96 (1H, m), 2.10–2.21 (1H, m), 2.55–2.69 (1H, m), 2.78 (3H, s), 2.81 (3H, s), 3.44–3.56 (1H, m), 4.09–4.27 (2H, m). ^{13}C NMR (D_2O): δ 13.26, 18.83, 30.06, 34.56, 38.73, 40.29, 60.19, 61.81, 166.20, 180.88. Anal. ($\text{C}_{12}\text{H}_{23}\text{NO}_6$) C, H, N.

3-((Cyclopropanecarbonyloxy)-1-methylpropyl)dimethylammonium Oxalate (5j). **5j** was prepared as described for **5h** from 3-(dimethylamino)butan-1-ol (**7**) (300 mg, 2.56 mmol) and cyclopropanecarbonyl chloride (0.26 mL, 2.8 mmol). The amino ester **5j** was isolated as the free amine (375 mg, 79%). The product was a colorless oil. The oxalate salt **5j** was prepared as described for **5b** from oxalic acid (53 mg, 0.59 mmol) and the free amine of **5j** (100 mg, 0.54 mmol). The colorless crystals obtained were recrystallized from $\text{CH}_2\text{Cl}_2\text{-Et}_2\text{O}$, affording 77.2 mg (52%). Mp: 116.8–117.7 °C. ^1H NMR (D_2O): δ 0.94–0.97 (4H, m), 1.32 (3H, d, $J = 6.7$ Hz), 1.64–1.72 (1H, m), 1.84–1.95 (1H, m), 2.09–2.19 (1H, m), 2.78 (3H, s), 2.81 (3H, s), 3.46–3.57 (1H, m), 4.08–4.16 (1H, m), 4.19–4.27 (1H, m). ^{13}C NMR (D_2O): δ 9.23, 13.06, 13.25, 30.08, 38.53, 40.33, 60.06, 61.82, 166.19, 178.38. Anal. ($\text{C}_{12}\text{H}_{21}\text{NO}_6$) C, H, N.

3-((Cyclobutanecarbonyloxy)-1-methylpropyl)dimethylammonium Oxalate (5k). **5k** was prepared as described for **5h** from 3-(dimethylamino)butan-1-ol (**7**) (300 mg, 2.56 mmol) and cyclobutanecarbonyl chloride (0.30 mL, 2.8 mmol). The amino ester **5j** was isolated as the free amine (375 mg, 74%). The product was a colorless oil. The oxalate salt **5k** was prepared as described for **5b** from oxalic acid (50 mg, 0.55 mmol) and the free amine of **5k** (100 mg, 0.50 mmol). The colorless crystals obtained were recrystallized from $\text{CH}_2\text{Cl}_2\text{-Et}_2\text{O}$, affording 106 mg (73%). Mp: 100.1–100.8 °C. ^1H NMR (CDCl_3): δ 1.38 (3H, d, $J = 6.7$ Hz), 1.70–1.82 (1H, m), 1.86–2.08 (2H, m), 2.15–2.34 (5H, m), 2.77 (6H, s), 3.09–3.20 (1H, m), 3.45–3.56 (1H, m), 4.07–4.25 (2H, m). ^{13}C NMR (CDCl_3): δ 13.49, 18.50, 25.33, 25.37, 30.20, 37.91, 39.24, 58.93, 60.34, 163.40, 175.29. Anal. ($\text{C}_{13}\text{H}_{23}\text{NO}_6$) C, H, N.

3-((Benzoyloxy)-1-methylpropyl)dimethylammonium Chloride (5l). 3-(Dimethylamino)butan-1-ol (200 mg, 1.71 mmol) was dissolved in dry CH_2Cl_2 (8 mL) and cooled to 0 °C. Benzoyl chloride (0.22 mL, 1.9 mmol) was added slowly, and the mixture was stirred at room temperature for 4 h. The solvent was evaporated and the oily residue left at 4 °C overnight, whereby the oil crystallized. The pink crystals were washed twice with Et_2O ,

affording 284 mg (64%) of **5l** as colorless crystals. An analytic portion was recrystallized from $\text{EtOH-Et}_2\text{O}$ and then $\text{CH}_2\text{Cl}_2\text{-Et}_2\text{O}$. Mp: 99.9–100.7 °C. ^1H NMR (CDCl_3): δ 1.50 (3H, d, $J = 6.6$ Hz), 1.89–1.98 (1H, m), 2.59–2.69 (1H, m), 2.75 (3H, d, $J = 5.0$ Hz), 2.77 (3H, d, $J = 5.0$ Hz), 3.44–3.54 (1H, m), 4.37–4.54 (2H, m), 7.42–7.47 (2H, m), 7.55–7.61 (1H, m), 7.99–8.02 (2H, m). ^{13}C NMR (CDCl_3): δ 13.78, 30.26, 38.49, 39.73, 59.24, 60.96, 128.69, 129.42, 129.74, 133.58, 166.38. Anal. ($\text{C}_{13}\text{H}_{20}\text{ClNO}_2$) C, H, N.

Enantiomeric Purity. To a 0.1 M solution of (*R*)-**5d**, (*S*)-**5d**, or racemic **5d** in CDCl_3 was added 2.2 equiv of (*R*)-(-)-2,2,2-trifluoro-1-(9-anthryl)-ethanol, and the ^1H NMR experiments were run within 2 h. The enantiomeric purities of (*R*)-**5d** and (*S*)-**5d** were determined from the duplets present at δ 0.811 ((*R*)-**5d**) and δ 0.821 ((*S*)-**5d**), and both enantiomers were found to be optically pure. The enantiomeric excess was estimated to be >95% with an inherent accuracy as expected from peak measurements. See Supporting Information for ^1H NMR spectra.

Pharmacology. Materials. [^3H]-(\pm)-Epibatidine ([^3H]epibatidine) and [^3H]methyllycaconitine ([^3H]MLA) were purchased from NEN (Zaventem, Belgium) and Tocris Cookson (Bristol, U.K.), respectively. Collagenase type 1A, gentamicin, tricaine (3-aminobenzoic acid ethyl ester methanesulfonate), and acetylcholine were obtained from Sigma-Aldrich, Denmark A/S. The human embryonic kidney (HEK) 293 cell lines stably expressing the rat $\alpha_3\beta_4$ and $\alpha_4\beta_4$ nAChR were generous gifts from Drs. K. Kellar and Y. Xiao (Georgetown University School of Medicine, Washington, DC), and a HEK293 cell line stably expressing rat $\alpha_4\beta_2$ nAChR was kindly provided by Dr. Joe Henry Steinbach (Washington University School of Medicine, St. Louis, MO). The cDNAs encoding the rat α_7 nAChR and the mouse 5-HT_{3A} receptor used to construct the $\alpha_7/5\text{-HT}_3$ chimera were kind gifts from Drs. James W. Patrick (Baylor College of Medicine, Houston, TX) and David J. Julius (University of California, San Francisco, CA), respectively.

Cell Culture. All cell lines were maintained at 37 °C in a humidified 5% CO_2 incubator in Dulbecco's modified Eagle medium supplemented with penicillin (100 U/mL), streptomycin (100 $\mu\text{g/mL}$), and 10% fetal calf serum. HEK293 cells stably expressing $\alpha_4\beta_2$, $\alpha_3\beta_4$, and $\alpha_4\beta_4$ nAChRs were cultured in medium containing G418 (0.5, 0.7, and 0.7 mg/mL, respectively).

[^3H]Epibatidine Binding. The [^3H]epibatidine binding experiments were performed as previously described.^{25,26} Briefly, the $\alpha_4\beta_2$, $\alpha_3\beta_4$, and $\alpha_4\beta_4$ cell lines were harvested and scraped into assay buffer [140 mM NaCl, 1.5 mM KCl, 2 mM CaCl_2 , 1 mM MgSO_4 , 25 mM HEPES (pH 7.4)], homogenized with a Polytron for 10 s, and centrifuged for 20 min at 50000g. Cell pellets were resuspended in fresh assay buffer, homogenized, and centrifuged at 50,000g for another 20 min. Cells were resuspended in assay buffer and incubated with [^3H]epibatidine at concentrations of 20 pM ($\alpha_4\beta_2$ and $\alpha_4\beta_4$) or 50 pM ($\alpha_3\beta_4$) in the presence of various concentrations of the test compounds in a total assay volume of 1 mL. Nonspecific binding was determined in assays with 5 mM (*S*)-nicotine. The assay mixtures were incubated for 4 h at room temperature while shaking, and binding was terminated by filtration through Whatman GF/C filters presoaked in 0.2% polyethylenimine using a 48-well cell harvester and subsequent washing with 3×4 mL of ice-cold isotonic NaCl solution. The filters were dried, 3 mL of Opti-Fluor (PerkinElmer, Boston, MA) was added, and the amount of bound radioactivity was determined in a scintillation counter. The binding experiments were performed in duplicate at least three times for each compound.

[^3H]MLA Binding. The [^3H]MLA binding experiments were performed as previously described.^{25,26} Briefly, 2×10^6 cells were split into a 15 cm tissue culture plate a day prior to transfection and transfected with 10 μg of $\alpha_7/5\text{-HT}_3\text{-pCDNA3}$ using Polyfect as a DNA carrier according to the protocol by the manufacturer (Qiagen, Hilden, Germany). The day after the transfection the medium was changed, and the following day cells were scraped into homogenization buffer, homogenized for 10 s in 30 mL of homogenization buffer [50 mM Tris-HCl (pH 7.2)] using a Polytron, and centrifuged for 20 min at 50000g. The resulting pellet were

homogenized in 30 mL of homogenization buffer and centrifuged again. The pellets were resuspended in PBS, and the cell membranes were incubated with 0.5 nM [^3H]methyllycaconitine and various concentrations of the test compounds in a total assay volume of 2 mL. Nonspecific binding was determined in reactions with 5 mM (*S*)-nicotine. The assay mixtures were incubated for 2.5 h at room temperature while shaking, and binding was terminated by filtration through GF/C filters presoaked in a 0.2% polyethylenimine solution using a 48-well cell harvester and subsequent washing with 3×4 mL of ice-cold isotonic NaCl solution. The filters were dried, 3 mL of Opti-Fluor was added, and the amount of bound radioactivity was determined in a scintillation counter. The binding experiments were performed in duplicate at least three times for each compound.

Data Analysis of Binding Experiments. Data from the binding experiments were fitted to the equation % bound = 100% bound / (1 + ([L]/IC₅₀)^{*n*}), and *K*_i values were determined using the Cheng–Prusoff equation $K_i = \text{IC}_{50} / (1 + [L]/K_D)$, where [L] is the radioligand concentration, *n* the Hill coefficient, and *K*_D the dissociation constant.

FLIPR Membrane Potential (FMP) Blue Assay. The compounds were characterized functionally at the $\alpha_3\beta_4$ -HEK293 cell line⁸⁵ in the FMP assay essentially as previously described.^{25,26} The cells were split into poly-D-lysine-coated black 96-well plates with clear bottom (BD Biosciences, Bedford, MA). After 16–24 h, the medium was aspirated, the wells were washed once with 100 μL of Krebs buffer [140 mM NaCl, 4.7 mM KCl, 2.5 mM CaCl₂, 1.2 mM MgCl₂, 11 mM HEPES, 10 mM D-Glucose, pH 7.4], and 100 μL of Krebs buffer supplemented with the FMP dye (Molecular Devices, Crawley, U.K.) was added to each well. The plate was incubated at 37 °C in a humidified 5% CO₂ incubator for 30 min and assayed in a NOVostar plate reader (BMG Labtechnologies) measuring emission [in fluorescence units (FU)] at 560 nm caused by excitation at 530 nm before and up to 1 min after addition of 33 μL of agonist solution. The experiments were performed in duplicate at least three times for each compound. Concentration–response curves for agonists in the FMP assay were constructed on the basis of the maximal responses at different concentrations of the respective ligands. Data from the FMP experiments were fitted to the simple mass equation: $R = R_{\text{basal}} + [R_{\text{max}} / (1 + (\text{EC}_{50}/[\text{A}])^n)]$, where [A] is the concentration of agonist, *n* the Hill coefficient, and *R* the response. Curves were generated by nonweighted least-squares fits using the program KaleidaGraph, version 3.6 (Synergy Software, Reading, PA).

Xenopus Oocyte Preparation. Female *Xenopus laevis* frogs were obtained from Nasco (Fort Atkinson, WI) and treated using standard protocols approved by NeuroSearch's Animal Care and Use Committee. Frogs were anesthetized with tricaine (0.28% in deionized water), and sections of one ovary (generally three to four lobes) were surgically removed and placed in low-Ca²⁺ Barth's solution (90 mM NaCl, 1 mM KCl, 0.66 mM NaNO₃, 2.4 mM NaHCO₃, 0.82 mM MgCl₂, 10 mM HEPES, and 100 $\mu\text{g}/\text{mL}$ gentamicin, final pH 7.55). The anesthetized frog was sacrificed after the operation by decapitation. The isolated ovary sections were opened using blunt dissection and rinsed in low-Ca²⁺ Barth's solution. To remove the follicular layer, the ovary sections were incubated in collagenase (Company, 2 mg/mL in low-Ca²⁺ Barths' solution) for 1–2 h at room temperature. Oocytes not defolliculated by the collagenase treatment were manually defolliculated. Hereafter, the oocytes were maintained at 17 °C in normal Barth's solution (90 mM NaCl, 1 mM KCl, 0.66 mM NaNO₃, 2.40 mM NaHCO₃, 0.74 mM CaCl₂, 0.82 mM MgCl₂, 10 mM HEPES, and 100 $\mu\text{g}/\text{mL}$ gentamicin, final pH 7.55). As an alternative source of oocytes, defolliculated oocytes were acquired and shipped directly from Ecocyte Bioscience (Castrop-Rauxel, Germany).

Cloning of the human α_3 , α_4 , α_7 , β_2 , and β_4 nAChR subunits and transcription into cRNA were performed as described previously.⁸⁶ Defolliculated oocytes were injected with a total of 40–50 ng of cRNA encoding the human α_7 subunit, human α_3 and β_4 subunits, or human α_4 and β_2 subunits, respectively. For $\alpha_3\beta_4$ nAChRs the cRNAs were injected as a 1:1 mixture, whereas $\alpha_4\beta_2$

cRNAs were injected as a 4:1 mixture in order to obtain a predominant expression of the low sensitivity form.

Oocyte Recording Conditions and Experimental Protocols.

Recordings were made using two-electrode voltage clamp by using a Geneclamp 500B amplifier with a bath clamp configuration in combination with a Digidata 1322A interface (both Molecular Devices, Sunnyvale, CA). Electrodes were made from bososilicate glass (1.5 mm o.d., 1.1 mm i.d.) and were filled with 3 M KCl. The impedance of the current-passing electrode was 0.5–2 M Ω . All experiments were conducted at a holding potential of –60 mV in an Oocyte Ringer's (OR) solution (90 mM NaCl, 2.5 mM KCl, 2.5 mM CaCl₂, 1 mM MgCl₂, and 5 mM HEPES, final pH 7.4). Oocytes were placed in a custom-made diamond-shaped recording chamber, which were continuously perfused at a rate of 1.5 mL/min with OR by using a peristaltic pump. Agonists, dissolved in OR, were applied through a glass capillary applicator (2.0 mm o.d./1.5 mm i.d.) placed in vicinity of the oocyte. Precise time controlled application was controlled by virtue of a Gilson 231 XL autosampler (Gilson, Inc., Middleton, WI) with the injection port connected to the applicator tube through Teflon-tubing ($1/16$ in. o.d. /0.25 mm i.d.), and the flow (2.5 mL/min) was created by the use of syringe pumps (Gilson 402, Gilson, Inc.). The timing of agonist applications was controlled by using the 735 Sampler Software (Gilson, Inc.), which was also used to trigger recording protocols defined by Clampex software (Molecular Devices, Sunnyvale, CA). The duration of agonist exposure was 12 s, and the interval between agonist applications was 5 min. Response stability was assessed through multiple applications of a saturating concentration of acetylcholine (10 mM for α_7 nAChR, 1 mM for $\alpha_3\beta_4$ and $\alpha_4\beta_2$ nAChRs) after which increasing concentrations of test agonists were applied. Responses of test agonists were quantified by measuring the amplitude of the response peak relative to the baseline current (Clampfit software, Molecular Devices, Sunnyvale, CA) and were normalized to the saturating acetylcholine response in the same oocyte.

Data from the oocyte experiments were fitted to the equation $R = R_{\text{basal}} + [R_{\text{max}} / (1 + (\text{EC}_{50}/[\text{A}])^n)]$, where [A] is the concentration of agonist, *n* the Hill coefficient, and *R* the response. Curves were generated by nonweighted least-squares fits using the Prism software (GraphPad Software, La Jolla, CA). Fitting parameters were not constrained except that the *R*_{basal} parameter was set equal to 0.

Acknowledgment. Drs. James W. Patrick and David J. Julius are thanked for their kind gifts of nAChR and 5-HT_{3A} receptor cDNAs. Drs. Ken Kellar and Yingxian Xiao are thanked for generously providing us with the $\alpha_3\beta_4$ and $\alpha_4\beta_4$ nAChR cell lines, and Dr. Joe Henry Steinbach is thanked for providing us with the $\alpha_4\beta_2$ -HEK293 cell line. Finally, Prof. Dan Stærk is thanked for helping in the development of a suitable procedure for determination of enantiomeric purity. This work was supported by the Lundbeck Foundation, the Carlsberg Foundation, and the Danish Medical Research Council.

Supporting Information Available: Data from microanalysis for all final compounds; spectral data of compounds (*R*)-7, 8, 9 and the free amines of 5a–k; ¹H NMR spectra of 5d, (*R*)-5d and (*S*)-5d with 2.2 equiv of (*R*)-(–)-2,2,2-trifluoro-1-(9-anthryl)-ethanol in CDCl₃. This material is available free of charge via the Internet at <http://pubs.acs.org>.

References

- (1) Gotti, C.; Zoli, M.; Clementi, F. Brain nicotinic acetylcholine receptors: native subtypes and their relevance. *Trends Pharmacol. Sci.* **2006**, *27*, 482–491.
- (2) Jensen, A. A.; Frølund, B.; Liljefors, T.; Krosgaard-Larsen, P. Neuronal nicotinic acetylcholine receptors: structural revelations, target identifications, and therapeutic inspirations. *J. Med. Chem.* **2005**, *48*, 4705–4745.
- (3) Karlin, A. Emerging structure of the nicotinic acetylcholine receptors. *Nat. Rev. Neurosci.* **2002**, *3*, 102–114.

- (4) Le Novère, N.; Changeux, J. P. Molecular evolution of the nicotinic acetylcholine-receptor. An example of multigene family in excitable cells. *J. Mol. Evol.* **1995**, *40*, 155–172.
- (5) Romanelli, M. N.; Gratteri, P.; Guandalini, L.; Martini, E.; Bonaccini, C.; Gualtieri, F. Central nicotinic receptors: structure, function, ligands, and therapeutic potential. *ChemMedChem* **2007**, *2*, 746–767.
- (6) Girod, R.; Barazangi, N.; McGehee, D.; Role, L. W. Facilitation of glutamatergic neurotransmission by presynaptic nicotinic acetylcholine receptors. *Neuropharmacology* **2000**, *39*, 2715–2725.
- (7) Kenny, P. J.; File, S. E.; Neal, M. J. Evidence for a complex influence of nicotinic acetylcholine receptors on hippocampal serotonin release. *J. Neurochem.* **2000**, *75*, 2409–2414.
- (8) Seth, P.; Cheeta, S.; Tucci, S.; File, S. E. Nicotinic-serotonergic interactions in brain and behaviour. *Pharmacol., Biochem. Behav.* **2002**, *71*, 795–805.
- (9) Ueda, M.; Iida, Y.; Kitamura, Y.; Kawashima, H.; Ogawa, M.; Magata, Y.; Saji, H. 5-Iodo-A-85380, a specific ligand for $\alpha_4\beta_2$ nicotinic acetylcholine receptors, prevents glutamate neurotoxicity in rat cortical cultured neurons. *Brain Res.* **2008**, *1199*, 46–52.
- (10) Grady, S. R.; Salminen, O.; Laverty, D. C.; Whiteaker, P.; McIntosh, J. M.; Collins, A. C.; Marks, M. J. The subtypes of nicotinic acetylcholine receptors on dopaminergic terminals of mouse striatum. *Biochem. Pharmacol.* **2007**, *74*, 1235–1246.
- (11) Janhunen, S.; Ahtee, L. Differential nicotinic regulation of the nigrostriatal and mesolimbic dopaminergic pathways: implications for drug development. *Neurosci. Biobehav. Rev.* **2007**, *31*, 287–314.
- (12) Dehkordi, O.; Millis, R. M.; Dennis, G. C.; Jazini, E.; Williams, C.; Hussain, D.; Jayam-Trouth, A. Expression of alpha-7 and alpha-4 nicotinic acetylcholine receptors by GABAergic neurons of rostral ventral medulla and caudal pons. *Brain Res.* **2007**, *1185*, 95–102.
- (13) Rollema, H.; Chambers, L. K.; Coe, J. W.; Glowa, J.; Hurst, R. S.; Lebel, L. A.; Lu, Y.; Mansbach, R. S.; Mather, R. J.; Rovetti, C. C.; Sands, S. B.; Schaeffer, E.; Schulz, D. W.; Tingley, F. D., III; Williams, K. E. Pharmacological profile of the $\alpha_4\beta_2$ nicotinic acetylcholine receptor partial agonist varenicline, an effective smoking cessation aid. *Neuropharmacology* **2007**, *52*, 985–994.
- (14) Fujita, M.; Ichise, M.; Zoghbi, S. S.; Liow, J.-S.; Ghose, S.; Vines, D. C.; Sangare, J.; Lu, J.-Q.; Cropley, V. L.; Iida, H.; Kim, K. M.; Cohen, R. M.; Bara-Jimenez, W.; Ravina, B.; Innis, R. B. Widespread decrease of nicotinic acetylcholine receptors in Parkinson's disease. *Ann. Neurol.* **2006**, *59*, 174–177.
- (15) Gotti, C.; Clementi, F. Neuronal nicotinic receptors: from structure to pathology. *Prog. Neurobiol.* **2004**, *74*, 363–396.
- (16) Oddo, S.; LaFerla, F. M. The role of nicotinic acetylcholine receptors in Alzheimer's disease. *J. Physiol. (Paris)* **2006**, *99*, 172–179.
- (17) Paterson, D.; Nordberg, A. Neuronal nicotinic receptors in the human brain. *Prog. Neurobiol.* **2000**, *61*, 75–111.
- (18) Kulak, J. M.; Fan, H.; Schneider, J. S. β_2^* and β_4^* nicotinic acetylcholine receptor expression changes with progressive parkinsonism in non-human primates. *Neurobiol. Dis.* **2007**, *27*, 312–319.
- (19) Marini, C.; Guerrini, R. The role of the nicotinic acetylcholine receptors in sleep-related epilepsy. *Biochem. Pharmacol.* **2007**, *74*, 1308–1314.
- (20) Gotti, C.; Riganti, L.; Vailati, S.; Clementi, F. Brain neuronal nicotinic receptors as new targets for drug discovery. *Curr. Pharm. Des.* **2006**, *12*, 407–428.
- (21) Picciotto, M. R.; Caldarone, B. J.; Brunzell, D. H.; Zachariou, V.; Stevens, T. R.; King, S. L. Neuronal nicotinic acetylcholine receptor subunit knock-out mice: physiological and behavioral phenotypes and possible clinical implications. *Pharm. Ther.* **2001**, *92*, 89–108.
- (22) Hilf, R. J. C.; Dutzler, R. X-ray structure of a prokaryotic pentameric ligand-gated ion channel. *Nature* **2008**, *452*, 375.
- (23) Brejc, K.; van Dijk, W. J.; Klaassen, R. V.; Schuurmans, M.; van der Oost, J.; Smit, A. B.; Sixma, T. K. Crystal structure of an ACh-binding protein reveals the ligand-binding domain of nicotinic receptors. *Nature* **2001**, *411*, 269–276.
- (24) Dellisanti, C. D.; Yao, Y.; Stroud, J. C.; Wang, Z.-Z.; Chen, L. Crystal structure of the extracellular domain of nAChR α_1 bound to α -bungarotoxin at 1.94 Å resolution. *Nat. Neurosci.* **2007**, *10* (8), 953–962.
- (25) Jensen, A. A.; Mikkelsen, I.; Frølund, B.; Frydenvang, K.; Brehm, L.; Jaroszewski, J. W.; Bräuner-Osborne, H.; Falch, E.; Krosgaard-Larsen, P. Carbamoylcholine homologs: synthesis and pharmacology at nicotinic acetylcholine receptors. *Eur. J. Pharmacol.* **2004**, *497*, 125–137.
- (26) Jensen, A. A.; Mikkelsen, I.; Frølund, B.; Bräuner-Osborne, H.; Falch, E.; Krosgaard-Larsen, P. Carbamoylcholine homologs: novel and potent agonists at neuronal nicotinic acetylcholine receptors. *Mol. Pharmacol.* **2003**, *64*, 865–875.
- (27) Adamson, D. W. Aminoalkyl tertiary carbinols and derived products. Part II. 3-Amino-1-1-di-2'-thienyl-alkan-1-ols and -alken-1-enes. *J. Chem. Soc.* **1950**, 885–890.
- (28) Hess, U.; Dunkel, S.; Mueller, B. Synthesis of β -amino acid derivatives via reductive amination of unsaturated carboxylic acid derivatives with dimcarb (dimethylamine-carbon dioxide adduct). *Pharmazie* **1993**, *48*, 591–597.
- (29) Negi, S.; Yamanaka, M.; Sugiyama, I.; Komatsu, Y.; Sasho, M.; Tsuruoka, A.; Kamada, A.; Tsukada, I.; Hiruma, R.; Katsu, K.; Machida, Y. Studies on orally-active cephalosporins. I. Synthesis and structure-activity relationships of new 3-substituted carbamoyloxymethyl cephalosporins. *J. Antibiot.* **1994**, *47*, 1507–1525.
- (30) Combrink, K. D.; Denton, D. A.; Harran, S.; Ma, Z.; Chapo, K.; Yan, D.; Bonventre, E.; Roche, E. D.; Doyle, T. B.; Robertson, G. T.; Lynch, A. S. New C25 carbamate rifamycin derivatives are resistant to inactivation by ADP-ribosyl transferases. *Bioorg. Med. Chem. Lett.* **2007**, *17*, 522–526.
- (31) Couty, F.; Evano, G.; Vargas-Sanchez, M.; Bouzas, G. Practical asymmetric preparation of azetidine-2-carboxylic acid. *J. Org. Chem.* **2005**, *70*, 9028–9031.
- (32) Rutjes, F. P. J. T.; Tjen, K. C. M. F.; Wolf, L. B.; Karstens, W. F. J.; Schoemaker, H. E.; Hiemstra, H. Selective azetidine and tetrahydropyridine formation via Pd-catalyzed cyclizations of allene-substituted amines and amino acids. *Org. Lett.* **1999**, *1*, 717–720.
- (33) Barluenga, J.; Fernández-Mari, F.; Viado, A. L.; Aguilar, E.; Olano, B. Diastereoselective synthesis of enantiomerically pure polysubstituted azetidines from 1,3-amino alcohols with three chiral centers. *J. Org. Chem.* **1996**, *61*, 5659–5662.
- (34) de Figueiredo, R. M.; Fröhlich, R.; Christmann, M. *N,N'*-Carbonyl-dimimidazole-mediated cyclization of amino alcohols to substituted azetidines and other N-heterocycles. *J. Org. Chem.* **2006**, *71*, 4147–4154.
- (35) Hillier, M. C.; Chen, C.-Y. A one-pot preparation of 1,3-disubstituted azetidines. *J. Org. Chem.* **2006**, *71*, 7885–7887.
- (36) Dejaeger, Y.; Kuz'menok, N. M.; Zvonok, A. M.; De Kimpe, N. The chemistry of azetidin-3-ones, oxetan-3-ones, and thietan-3-ones. *Chem. Rev.* **2002**, *102*, 29–60.
- (37) Forbes, J. E.; Saicic, R. N.; Zard, S. Z. New radical reactions of *S*-alkoxycarbonyl xanthates. Total synthesis of (\pm)-cinnamofide and (\pm)-methylenolactocin. *Tetrahedron* **1999**, *55*, 3791–3802.
- (38) Huang, H.; Iwasawa, N.; Mukaiyama, T. A convenient method for the construction of β -lactam compounds from β -amino acids using 2-chloro-1-methylpyridinium iodide as condensing reagent. *Chem. Lett.* **1984**, 1465–1466.
- (39) Nilsson, B. M.; Ringdahl, B.; Hacksell, U. β -Lactam analogs of oxotremorine: 3- and 4-methyl-substituted 2-azetidiones. *J. Med. Chem.* **1990**, *33*, 580–584.
- (40) Ojima, I.; Zhao, M. Z.; Yamato, T.; Nakahashi, K.; Yamashita, M.; Abe, R. Azetidines and bisazetidines. Their synthesis and use as the key intermediates to enantiomerically pure diamines, amino-alcohols, and polyamines. *J. Org. Chem.* **1991**, *56*, 5263–5277.
- (41) Van Brabant, W.; Dejaeger, Y.; Van Landeghem, R.; De Kimpe, N. Reduction of 4-(haloalkyl)azetidin-2-ones with LiAlH_4 as a powerful method for the synthesis of stereodefined aziridines and azetidines. *Org. Lett.* **2006**, *8*, 1101–1104.
- (42) Yamashita, M.; Ojima, I. Effective route to azetidines from azetidin-2-ones using hydroalanes as specific reducing agents. *J. Am. Chem. Soc.* **1983**, *105*, 6339–6342.
- (43) Bandini, E.; Favi, G.; Martelli, G.; Panunzio, M.; Piersanti, G. A trans-stereoselective synthesis of 3-halo-4-alkyl(aryl)-NH-azetidin-2-ones. *Org. Lett.* **2000**, *2*, 1077–1079.
- (44) Evans, P. A.; Holmes, A. B.; McGeary, R. P.; Nadin, A.; Russell, K.; O'Hanlon, P. J.; Pearson, N. D. New methodology for the synthesis of unsaturated 8-, 9- and 10-membered lactams. *J. Chem. Soc., Perkin Trans. 1* **1996**, 123–138.
- (45) Vaughan, W. R.; Klonowski, R. S.; McElhinney, R. S.; Millward, B. B. Synthesis of potential anticancer agents. V. Azetidines. *J. Org. Chem.* **1961**, *26*, 138.
- (46) Thompson, H. W.; Swistok, J. Enamines of 3,3-dimethylazetidine. *J. Org. Chem.* **1981**, *46*, 4907–4911.
- (47) Boger, D. L.; Patel, M. Activation and coupling of pyrrole-1-carboxylic acid in the formation of pyrrole *N*-carbonyl compounds: pyrrole-1-carboxylic acid anhydride. *J. Org. Chem.* **1987**, *52*, 2319–2323.
- (48) Kinas, R.; Pankiewicz, K.; Stec, W. J.; Farmer, P. B.; Foster, A. B.; Jarman, M. Synthesis and absolute configuration of optically active forms of 2-[bis(2-chloroethyl)amino]-4-methyltetrahydro-2*H*-1,3,2-oxazaphosphorine 2-oxide(4-methylcyclophosphamide). *J. Org. Chem.* **1977**, *42*, 1650–1652.
- (49) Yamagishi, T.; Fujii, K.; Shibuya, S.; Yokomatsu, T. Asymmetric synthesis of phosphonic acid analogues for acylcarnitine. *Tetrahedron* **2006**, *62*, 54–65.
- (50) Paquette, L. A.; Mitzel, T. M.; Isaac, M. B.; Crasto, C. R.; Schomer, W. W. Diastereoselection during 1,2-addition of the allylindium reagent to α -thia and α -amino aldehydes in aqueous and organic solvents. *J. Org. Chem.* **1997**, *62*, 8960.
- (51) Jeffery, G. H.; Vogel, A. I. Physical properties and chemical constitution. 18. 3-Membered and 4-membered carbon rings. *J. Chem. Soc.* **1948**, 1804–1809.

- (52) Bailey, W. J.; Hewitt, J. J. Pyrolysis of esters. 7. Influence of acid portion. *J. Org. Chem.* **1956**, *21*, 543–546.
- (53) Yasui, S. C.; Keiderling, T. A. Vibrational circular-dichroism of optically active cyclopropanes. 3. *trans*-2-Phenylcyclopropanecarboxylic acid derivatives and related compounds. *J. Am. Chem. Soc.* **1987**, *109*, 2311–2320.
- (54) Xiao, Y.; Baydyuk, M.; Wang, H. P.; Davis, H. E.; Kellar, K. J. Pharmacology of the agonist binding sites of rat neuronal nicotinic receptor subtypes expressed in HEK 293 cells. *Bioorg. Med. Chem. Lett.* **2004**, *14*, 1845–1848.
- (55) Sabey, K.; Paradiso, K.; Zhang, J.; Steinbach, J. H. Ligand binding and activation of rat nicotinic $\alpha_4\beta_2$ receptors stably expressed in HEK293 cells. *Mol. Pharmacol.* **1999**, *55*, 58–66.
- (56) Baker, E. R.; Zwart, R.; Sher, E.; Millar, N. S. Pharmacological properties of $\alpha_9\alpha_{10}$ nicotinic acetylcholine receptors revealed by heterologous expression of subunit chimeras. *Mol. Pharmacol.* **2004**, *65*, 453–460.
- (57) Davies, A. R. L.; Hardick, D. J.; Blagbrough, I. S.; Potter, B. V. L.; Wolstenholme, A. J.; Wonnacott, S. Characterisation of the binding of [³H]methyllycaconitine: a new radioligand for labelling α_7 -type neuronal nicotinic acetylcholine receptors. *Neuropharmacology* **1999**, *38*, 679–690.
- (58) Carbonnelle, E.; Sparatore, F.; Canu-Boido, C.; Salvagno, C.; Baldani-Guerra, B.; Terstappen, G.; Zwart, R.; Vijverberg, H.; Clementi, F.; Gotti, C. Nitrogen substitution modifies the activity of cytosine on neuronal nicotinic receptor subtypes. *Eur. J. Pharmacol.* **2003**, *471*, 85–96.
- (59) Chavez-Noriega, L. E.; Crona, J. H.; Washburn, M. S.; Urrutia, A.; Elliott, K. J.; Johnson, E. C. Pharmacological characterization of recombinant human neuronal nicotinic acetylcholine receptors $\alpha_2\beta_2$, $\alpha_2\beta_4$, $\alpha_3\beta_2$, $\alpha_3\beta_4$, $\alpha_4\beta_2$, $\alpha_4\beta_4$ and α_7 expressed in *Xenopus* oocytes. *J. Pharmacol. Exp. Ther.* **1997**, *280*, 346–356.
- (60) Fitch, R. W.; Xiao, Y.; Kellar, K. J.; Daly, J. W. Membrane potential fluorescence: a rapid and highly sensitive assay for nicotinic receptor channel function. *Proc. Natl. Acad. Sci. U.S.A.* **2003**, *100*, 4909–4914.
- (61) Stauderman, K. A.; Mahaffy, L. S.; Akong, M.; Velicelebi, G.; Chavez-Noriega, L. E.; Crona, J. H.; Johnson, E. C.; Elliott, K. J.; Gillespie, A.; Reid, R. T.; Adams, P.; Harpold, M. M.; Corey-Naev, J. Characterization of human recombinant neuronal nicotinic acetylcholine receptor subunit combinations $\alpha_2\beta_4$, $\alpha_3\beta_4$ and $\alpha_4\beta_4$ stably expressed in HEK293 cells. *J. Pharmacol. Exp. Ther.* **1998**, *284*, 777–789.
- (62) Le Novère, N.; Grutter, T.; Changeux, J. P. Models of the extracellular domain of the nicotinic receptors and of agonist- and Ca²⁺-binding sites. *Proc. Natl. Acad. Sci. U.S.A.* **2002**, *99*, 3210–3215.
- (63) Bairoch, A.; Apweiler, R.; Wu, C. H.; Barker, W. C.; Boeckmann, B.; Ferro, S.; Gasteiger, E.; Huang, H.; Lopez, R.; Magrane, M.; Martin, M. J.; Natale, D. A.; O'Donovan, C.; Redaschi, N.; Yeh, L. S. L. The universal protein resource (UniProt). *Nucleic Acids Res.* **2005**, *33*, D154–D159.
- (64) Celie, P. H. N.; Rossum-Fikkert, S. E.; van Dijk, W. J.; Brejc, K.; Smit, A. B.; Sixma, T. K. Nicotine and carbamylcholine binding to nicotinic acetylcholine receptors as studied in AChBP crystal structures. *Neuron* **2004**, *41*, 907–914.
- (65) Hansen, S. B.; Talley, T. T.; Radic, Z.; Taylor, P. Structural and ligand recognition characteristics of an acetylcholine-binding protein from *Aplysia californica*. *J. Biol. Chem.* **2004**, *279*, 24197–24202.
- (66) Hansen, S. B.; Sulzenbacher, G.; Huxford, T.; Marchot, P.; Taylor, P.; Bourne, Y. Structures of *Aplysia* AChBP complexes with nicotinic agonists and antagonists reveal distinctive binding interfaces and conformations. *EMBO J.* **2005**, *24*, 3635–3646.
- (67) Brady, G. P.; Stouten, P. F. W. Fast prediction and visualization of protein binding pockets with PASS. *J. Comput.-Aided Mol. Des.* **2000**, *14*, 383–401.
- (68) Grutter, T.; Le Novère, N.; Changeux, J. P. Rational understanding of nicotinic receptors drug binding. *Curr. Top. Med. Chem.* **2004**, *4*, 645–650.
- (69) Yuan, H. B.; Petukhov, P. A. Computational evidence for the ligand selectivity to the $\alpha_4\beta_2$ and $\alpha_3\beta_4$ nicotinic acetylcholine receptors. *Bioorg. Med. Chem.* **2006**, *14*, 7936–7942.
- (70) Parker, M. J.; Beck, A.; Luetje, C. W. Neuronal nicotinic receptor β_2 and β_4 subunits confer large differences in agonist binding affinity. *Mol. Pharmacol.* **1998**, *54*, 1132–1139.
- (71) Carroll, F. I.; Liang, F.; Navarro, H. A.; Briecaddy, L. E.; Abraham, P.; Damaj, M. I.; Martin, B. R. Synthesis, nicotinic acetylcholine receptor binding, and antinociceptive properties of 2-exo-2-(2'-substituted 5'-pyridinyl)-7-azabicyclo[2.2.1]heptanes. Epibatidine analogues. *J. Med. Chem.* **2001**, *44*, 2229–2237.
- (72) Che, C.; Petit, G.; Kotzyba-Hibert, F.; Bertrand, S.; Bertrand, D.; Grutter, T.; Goeldner, M. Syntheses and biological properties of cysteine-reactive epibatidine derivatives. *Bioorg. Med. Chem. Lett.* **2003**, *13*, 1001–1004.
- (73) Duan, G.; Smith, V. H.; Weaver, D. F. Characterization of aromatic–amide (side-chain) interactions in proteins through systematic ab initio calculations and data mining analyses. *J. Phys. Chem. A* **2000**, *104*, 4521–4532.
- (74) Anderson, D. J.; Arneric, S. P. Nicotinic receptor-binding of [³H]-cytosine, [³H]-nicotine and [³H]-methylcarbamylcholine in rat-brain. *Eur. J. Pharmacol.* **1994**, *253*, 261–267.
- (75) Punzi, J. S.; Banerjee, S.; Abood, L. G. Structure-activity-relationships for various *N*-alkylcarbamyl esters of choline with selective nicotinic cholinergic properties. *Biochem. Pharmacol.* **1991**, *41*, 465–467.
- (76) Søkilde, B.; Mikkelsen, I.; Stensbøl, T. B.; Andersen, B.; Ebdrup, S.; Krosgaard-Larsen, P.; Falch, E. Analogues of carbacholine: synthesis and relationship between structure and affinity for muscarinic and nicotinic acetylcholine receptors. *Arch. Pharm.* **1996**, *329*, 95–104.
- (77) Sullivan, J. P.; Donnelly-Roberts, D.; Briggs, C. A.; Anderson, D. J.; Gopalakrishnan, M.; Xue, I. C.; Piattoni-Kaplan, M.; Molinari, E.; Campbell, J. E.; McKenna, D. G.; Gunn, D. E.; Lin, N. H.; Ryther, K. B.; He, Y.; Holladay, M. W.; Wonnacott, S.; Williams, M.; Arneric, S. P. ABT-089 [2-methyl-3-(2-(*S*)-pyrrolidinylmethoxy)pyridine]. I. A potent and selective cholinergic channel modulator with neuroprotective properties. *J. Pharmacol. Exp. Ther.* **1997**, *283*, 235–246.
- (78) Chen, Y.; Sharples, T. J. W.; Phillips, K. G.; Benedetti, G.; Broad, L. M.; Zwart, R.; Sher, E. The nicotinic $\alpha_4\beta_2$ receptor selective agonist, TC-2559, increases dopamine neuronal activity in the ventral tegmental area of rat midbrain slices. *Neuropharmacology* **2003**, *45*, 334–344.
- (79) Rollema, H.; Coe, J. W.; Chambers, L. K.; Hurst, R. S.; Stahl, S. M.; Williams, K. E. Rationale, pharmacology and clinical efficacy of partial agonists of $\alpha_4\beta_2$ nACh receptors for smoking cessation. *Trends Pharmacol. Sci.* **2007**, *28*, 316–325.
- (80) Mihalak, K. B.; Carroll, F. I.; Luetje, C. W. Varenicline is a partial agonist at $\alpha_4\beta_2$ and a full agonist at α_7 neuronal nicotinic receptors. *Mol. Pharmacol.* **2006**, *70*, 801–805.
- (81) Slater, Y. E.; Houlihan, L. M.; Maskell, P. D.; Exley, R.; Bermúdez, I.; Lukas, R. J.; Valdivia, A. C.; Cassels, B. K. Halogenated cytosine derivatives as agonists at human neuronal nicotinic acetylcholine receptor subtypes. *Neuropharmacology* **2003**, *44*, 503–515.
- (82) Bosse, K.; Marineau, J.; Nason, D. M.; Fliri, A. J.; Segelstein, B. E.; Desai, K.; Volkmann, R. A. Expanding the medicinal chemistry toolbox: stereospecific generation of methyl group-containing propylene linkers. *Tetrahedron Lett.* **2006**, *47*, 7285–7287.
- (83) Jessen, C. U.; Selvig, H.; Valsborg, J. S. Synthesis of N-protected ¹⁴C-labelled (2*E*)-5-amino-5-methylhex-2-enoic acid analogues. *J. Labelled Compd. Radiopharm.* **2001**, *44*, 265–275.
- (84) Angle, S. R.; Belanger, D. S. Stereoselective synthesis of 3-hydroxyproline benzyl esters from N-protected β -aminoaldehydes and benzyl diazoacetate. *J. Org. Chem.* **2004**, *69*, 4361–4368.
- (85) Xiao, Y.; Meyer, E. L.; Thompson, J. M.; Surin, A.; Wroblewski, J.; Kellar, K. J. Rat α_3/β_4 subtype of neuronal nicotinic acetylcholine receptor stably expressed in a transfected cell line: pharmacology of ligand binding and function. *Mol. Pharmacol.* **1998**, *54*, 322–333.
- (86) Timmermann, D. B.; Grønlien, J. H.; Kohlhaas, K. L.; Nielsen, E. Ø.; Dam, E.; Jørgensen, T. D.; Ahring, P. K.; Peters, D.; Holst, D.; Christensen, J. K.; Malysz, J.; Briggs, C. A.; Gopalakrishnan, M.; Olsen, G. M. An allosteric modulator of the α_7 nicotinic acetylcholine receptor possessing cognition-enhancing properties in vivo. *J. Pharmacol. Exp. Ther.* **2007**, *323*, 294–307.